

CD44-dependent lymphoma cell dissemination: a cell surface CD44 variant, rather than standard CD44, supports in vitro lymphoma cell rolling on hyaluronic acid substrate and its in vivo accumulation in the peripheral lymph nodes

Shulamit B. Wallach-Dayana¹, Valentin Grabovsky², Jürgen Moll^{3,*}, Jonathan Sleeman³, Peter Herrlich³, Ronen Alon² and David Naor^{1,‡}

¹The Lautenberg Center for General and Tumor Immunology, The Hebrew University-Hadassah Medical School, Jerusalem, 91120 Israel

²Department of Immunology, The Weizmann Institute, Rehovot, 76100 Israel

³Forschungszentrum Karlsruhe, Institute of Toxicology and Genetics, Karlsruhe D-76021, Germany

*Present address: Pharmacia & Upjohn, via Pasteur 10, 1-20014 Nerviano (Milan), Italy

‡Author for correspondence (e-mail: naord@md2.huji.ac.il)

Accepted 25 June 2001

Journal of Cell Science 114, 3463-3477 (2001) © The Company of Biologists Ltd

SUMMARY

Cell motility is an essential element of tumor dissemination, allowing organ infiltration by cancer cells. Using mouse LB lymphoma cells transfected with standard CD44 (CD44s) cDNA (LB-TRs cells) or with the alternatively spliced CD44 variant CD44v4-v10 (CD44v) cDNA (LB-TRv cells), we explored their CD44-dependent cell migration. LB-TRv cells, but not LB-TRs or parental LB cells, bound soluble hyaluronic acid (HA) and other glycosaminoglycans (GAGs), and exclusively formed, under physiological shear force, rolling attachments on HA substrate. Furthermore, LB-TRv cells, but not LB-TRs cells or their parental LB cells, displayed accelerated local tumor formation and enhanced accumulation in the peripheral lymph nodes after s.c. inoculation. The aggressive metastatic behavior of i.v.-injected LB-TRV cells, when compared with that of other LB-transfectants, is attributed to more efficient

migration to the lymph nodes, rather than to local growth in the lymph node. Injection of anti-CD44 monoclonal antibody or of the enzyme hyaluronidase also prevented tumor growth in lymph nodes of BALB/c mice inoculated with LB-TRv cells. The enhanced in vitro rolling and enhanced in vivo local tumor growth and lymph node invasion disappeared in LB cells transfected with CD44v cDNA bearing a point mutation at the HA binding site, located at the distal end of the molecule constant region. These findings show that the interaction of cell surface CD44v with HA promotes cell migration both in vitro and in vivo, and they contribute to our understanding of the mechanism of cell trafficking, including tumor spread.

Key words: Adhesion molecules, CD44, Cell motility, Cell rolling, Hyaluronic acid, lymphoma cells

INTRODUCTION

Cell motility is a universal and essential facet of tumor dissemination, whereas, in a normal adult organism, this physiological activity is more limited (e.g. to cells of the immune system or cells involved in wound healing and tissue remodeling). While the function of selectins and integrins in supporting cell motility and homing has been well established (Springer, 1994), the role of cell surface CD44 only later attracted attention (Naor et al., 1997). Alternative splicing and/or post-translational modifications generate many CD44 isoforms. The large array of CD44 isoforms is mainly attributable to the insertion of amino acid sequences encoded by different combinations of 10 variant exons, into a membrane proximal position of the extracellular domain. Transcripts in which these variant exons are spliced out encode the most common and widely expressed 85 kDa isoform, known as standard CD44 (CD44s). The expression of CD44 isoforms

containing sequences encoded by the variant exons (CD44v) is tightly regulated and restricted to epithelial cells, cells undergoing activation or differentiation, as well as to some progressor tumors (Lesley et al., 1993; Naor et al., 1997).

The polymorphic nature of CD44 possibly contributes to its multifunctionality. For instance, CD44 molecules support cell migration (DeGrendele et al., 1997a), mediate T-cell signaling and activation (Taher et al., 1996; Lesley et al., 1993; Naor et al., 1997), as well as lymphocyte recirculation (Guo et al., 1994). CD44 is involved in cell-cell and cell-matrix interactions (Lesley et al., 1993; Naor et al., 1997) and in the presentation of cytokines and growth factors to high affinity receptors (Tanaka et al., 1993; Bennet et al., 1995). It is likely that the CD44 receptor interacts with many ligands, only some of which have been identified. The most solid evidence for CD44 ligands is that relating to glycosaminoglycans (GAGs), such as hyaluronic acid (HA). A single mutation at amino acid position 41 dramatically reduced the ligand binding capacity

of the human CD44 receptor (Peach et al., 1993). The affinity of the CD44 receptor for HA appears to depend on post-translational modifications (i.e. N- or O-glycosylations and GAG attachments; Lesley et al., 1995) as well as on specific structural changes in CD44 oligosaccharides (e.g. gain or loss of sialic acid; English et al., 1998; Skelton et al., 1998). Cells carrying CD44 may bind HA constitutively, not interact with HA at all, or do so upon activation, depending on low, high or intermediate levels of receptor glycosylation, respectively (Lesley et al., 1995; Lesley et al., 1993; Naor et al., 1997).

The migration of many types of tumors is CD44-dependent. As CD44 is a diverse family of molecules, which includes CD44s as well as CD44v isoforms, specific isoform(s) might be involved in the support of tumor spread. Indeed, it has been found that CD44v molecules, especially those containing variant exon number 6 (v6), are predominantly expressed on some (but not all) progressive and metastatic neoplasms (Naor et al., 1997), including the non-Hodgkin's lymphomas (Salles et al., 1993; Stauder et al., 1995). As mentioned above, it has been shown in an animal model that cell surface v6-containing CD44v supports the metastasis of a pancreatic adenocarcinoma cell line (Günthert et al., 1991). It was postulated that tumor cells, and especially lymphoma cells, resemble activated lymphocytes in their migratory properties and in the route of migration to the lymph nodes (Herrlich et al., 1993). In addition, it was reported that such activated lymphocytes express CD44v and its expression promotes accelerated lymphocyte proliferation following their stimulation (Moll et al., 1996). A possible mechanism for CD44v-promoted proliferation is the trapping of growth factors by this receptor (Bennett et al., 1995; Jones et al., 2000; Sherman et al., 1998). As mentioned above, CD44v seems to confer invasive properties (Günthert et al., 1991), perhaps, again, by capture of growth factors and their subsequent presentation to the relevant cell surface receptors (van der Voort et al., 1999) that activate the cytoskeleton.

All known CD44 isoforms carry a GAG binding motif. We previously showed that CD44v isoforms exhibit broader GAG binding specificity (which may reflect higher avidity) than CD44s (Sleeman et al., 1997), possibly due to the ability of CD44v to form cell surface clusters (Sleeman et al., 1996a). GAG binding may confer a number of different cellular functions, such as enhanced proliferation (Moll et al., 1996), or cell migration (DeGrendele et al., 1997a). To dissociate these effects, we decided to study how expression or lack of expression of CD44 alternatively spliced exons, which constitutively bind HA, influences the different tumor cell functions. To be independent of induced proliferation or induced alternative splicing, we transfected cDNAs driven by a constitutive promoter and selected clones expressing an equal level of the exogenous CD44v isoform. We report here that in the LB cell line, CD44v, but not CD44s, mediates GAG binding, rolling on HA substrate under physiological shear stress and migration of the tumor cells into lymphatic tissue upon subcutaneous (s.c.) injection. It should be emphasized, however, that in other cell lines CD44s can support cell rolling under shear stress (DeGrendele et al., 1997b). These properties disappear when the cell surface CD44v contains a mutation at the HA binding site located at the distal end of the molecule's constant region. These findings show for the first time that the CD44 variant, but not standard CD44, supports the rolling of the lymphoma cells and suggest that the variable region of the

cell surface CD44 receptor controls the ability of the constant region binding domain to support lymphoma cell migration *in vitro* and its accumulation in the lymph nodes *in vivo*.

MATERIALS AND METHODS

Mice

Five-to-six-week-old female BALB/c mice and nude mice of BALB/c origin were obtained from Harlan (Indianapolis, IN) and maintained under specific pathogen-free conditions in the Hadassah Medical School Animal Unit, Hebrew University, Jerusalem.

Cell cultures

LB T-cell lymphoma cells derived from a spontaneous tumor of a BALB/c mouse (Ruggiero et al., 1985) were cultivated in LB medium, consisting of a 1:1 mixture of RPMI-1640 and DCCM-1 media (Sigma, St Louis, MO), supplemented with 5% heat-inactivated fetal calf serum (FCS) (Sigma), 2 mM glutamine, 1 mM sodium pyruvate, 10 mM Hepes and 5×10^{-5} M β -mercaptoethanol. Hybridomas obtained from American type culture collection (ATCC) were grown in RPMI-1640 medium enriched with 10% FCS, and expanded in nude mice. Cell cultures were incubated at 37°C in 5% humidified CO₂. For FACS analysis, cells were stained with 3% FCS in PBS (FACS medium). The following antibiotics were used in the selective medium: 0.3 mg/ml Geneticin-G418 (GIBCO #41811; Life Technologies, Paisley, UK) and 0.5 mg/ml Zeomycin (Zeocin™ #R250-01; Invitrogen, Carlsbad, CA).

Monoclonal antibodies, enzymes and other reagents

The following rat anti-mouse pan CD44 monoclonal antibodies (mAbs) (constant region-specific) were produced from ATCC hybridomas: IM7.8.1 (IgG2b) (Trowbridge et al., 1982), KM81 (IgG2b) (Miyake et al., 1990) and KM114 (IgG1) (Miyake et al., 1990). The rat anti-mouse CD44v4 (10D1; IgG1) and rat anti-mouse CD44v6 (9A4; IgG1) were previously described (Weiss et al., 1997). The rat anti-mouse cell surface immunoglobulin idiotype (4D2; IgG2b), kindly provided by J. Haimovich, Tel Aviv University (Maloney et al., 1985), was used as an irrelevant isotype control. In addition, in the flow cytometry assay we used the following ATCC rat anti-mouse mAbs to analyze expression of cell adhesion molecules: anti-CD11a (M7/14; IgG2a) (Davignon et al., 1981), anti-CD11b (M1/70; Ig2a) (Springer et al., 1979), anti-CD18 (M18/2; IgG2a) (Sanchez-Madrid et al., 1983), MEL-14 (MEL-14.D54; IgG2a) (Gallatin et al., 1983) and anti-ICAM-1 (YN1/1.7; IgG2a) (Takei, 1985). The hybridomas were injected into the peritoneal cavity of nude mice and the mAbs were purified from the ascitic fluid by protein S-sepharose chromatography as described previously (Rochman et al., 2000). Biotin-conjugated anti-mouse CD44s was produced by biotinylation of KM81 mAb, as described (Yang et al., 1995). FITC-conjugated F(ab)₂ goat anti-rat (goat IgG (H and L)) was obtained from Jackson Immunoresearch, West Grove, PA. HRP-peroxidase-conjugated streptavidine and R- phycoerythrin-conjugated streptavidine were obtained from Jackson Immunoresearch. Biotinylated anti-bromodeoxyuridine (BrdU) antibody was obtained from Biotools International (Saco, Maine), Cy⁵-conjugated streptavidin was obtained from Jackson Immunoresearch, BrdU (B5002) and propidium iodide were purchased from Sigma. The following GAGs and enzymes were obtained from Sigma: hyaluronic acid (H5388), chondroitin 4, 6-sulfate C (CS) (C4384), keratan sulfate (KS) (K3001), heparin (H3393), heparan sulfate (HS) (H7641), heparinase (H2519) and hyaluronidase (H3757).

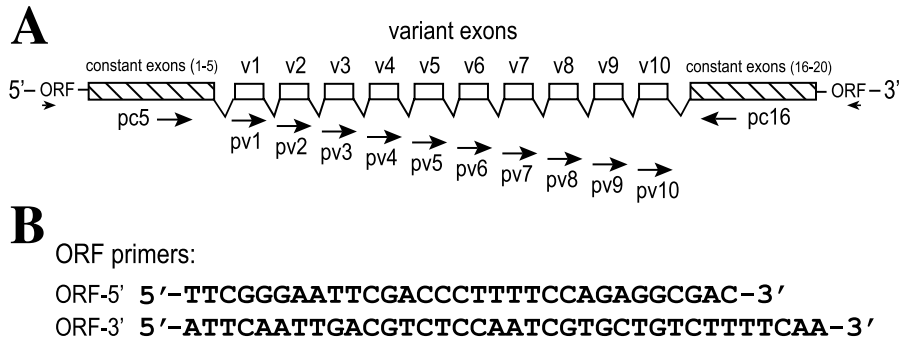
Construction of CD44v4-v10 and CD44s expression plasmids

CD44v4-v10 cDNA was synthesized from 500 ng polyadenylated

Fig. 1. Generation of LB-TRv transfectants.

(A) Schematic map of the CD44 gene.

Arrowheads mark the positions of 5'-ORF and 3'-ORF primers (sequence as shown in B) used to isolate the CD44v4-v10 cDNA from mouse keratinocytes. Arrows mark the positions and directions (sense →; anti-sense ←) of the primers (for sequence, see Rochman et al., 2000) used in the exon-specific RT-PCR analysis of LB cells transfected with isolated CD44v4-v10 cDNA (LB-TRv cells). Hatched bars denote 5' and 3' constant exons (excluding introns), open bars represent the variant exons, the lines connecting the exons depict intron sequences. Pc5 and pv1 to pv10 primers were used for exon-specific PCRs in combination with the 3' primer pc16, for analysis of mouse cDNA. (B) ORF-5' and ORF-3' primers.



RNA prepared from mouse keratinocytes (KLN205 from ATCC), using the oligonucleotide primers ORF-3' and ORF-5', which overlap the open reading frame of the 3' (nucleotide positions 58-80) and 5' (nucleotide positions 1216-1244) constant regions of the CD44 DNA (Zhou et al., 1989), as described in Fig. 1A,B. ORF-5' includes the *Eco*RI cloning site. After 30 PCR cycles (95°C, 45 seconds; 60°C, 1 minute; 72°C, 3 minutes), the amplification products were purified, using a Qiagen PCR product purification kit. Purified products were cloned into the pZeoSV vector (#V855-01, Invitrogen, Carlsbad, CA) to generate the pZeoSVCD44v4-v10 plasmid. CD44s cDNA was prepared as described (Tölg et al., 1993), and cloned into the *Eco*RI site of pZeoSV, resulting in the pZeoSVCD44s plasmid. The correctness of the insert was confirmed by sequencing.

Construction of an expression plasmid encoding a CD44 HA binding mutant

Site-directed mutagenesis by overlap extension, using two-step PCR was performed precisely as described (Ho et al., 1989), resulting in the replacement of arginine by alanine at position 43 of mouse CD44v4-v10 cDNA (for detailed graphical schematic description, see Ho et al., 1989). The flanking external primers (A: 5'-CGG, GAA, TTC, GAC, CCT, TTT, CCA, GA-3' and D: 5'-TTC, GTC, TCC, AAT, CGT, GCT, GTC, TT-3') were hybridized at each end of the target sequence (pZeoSVCD44v4-v10 expression construct). The internal primers (B: 5'-GAT, ACT, GTA, GGC, GCC, ATT, TTT, CTC, C-3' and C: 5'-GGA, GAA, AAA, TGG, CGC, CTA, CAG, TAT, C-3'), containing the mismatched bases, were hybridized at the site of the mutation. The HA binding site mutation was confirmed by dideoxy sequencing.

Generation of CD44 stable transfectants

Logarithmically growing LB cells were harvested, washed with RPMI-1640 medium and then resuspended in LB medium containing 20% FCS. A quantity of 20 µg from the following expression vectors was added to 800 µl of cell suspension (4×10⁶ cells per ml): empty pZeoSV vector (to generate transfectants designated LB-TRo cells), or pZeoSVCD44s, pZeoSVCD44v4-v10 and pZeoSVCD44v4-v10 mutated at the HA binding site (to generate transfectants designated LB-TRs, LB-TRv and LB-TRvM cells, respectively). Transfection was carried out by electroporation at 380 V and 500 µF, using a BIO-RAD, Gene Pulser (Bio Rad Laboratories, Hercules, CA). The cells were cultured in 6 ml LB medium containing 20% FCS, incubated for 24 hours and then grown in the same medium supplemented with 0.5 mg/ml Zeomycin to select for the transfected cells. Transfected cell clones were obtained by limiting dilution and cDNA expression was confirmed by exon-specific RT-PCR, by using the primers described previously (Rochman et al., 2000) and the primer orientations shown in Fig. 1A.

Generation of green fluorescence protein (GFP) stable transfectants

To detect dissemination of the lymphoma cells following their s.c. inoculation, LB, LB-TRs, LB-TRv and LB-TRvM cell lines were transfected with GFP-N1 expression vector (#6091-1, Clontech Laboratories, Palo Alto, CA), which contains jellyfish GFP cDNA (Chishima et al., 1997). The transfection was carried out as described above, except that 1 mg/ml G418 (GIBCO) was used for selection. Lymphoma cells expressing GFP were electronically sorted.

Flow cytometry

Lymphoma cell surface expression of CD44 was assessed by indirect immunofluorescence and analyzed by flow cytometry as described (Zahalka et al., 1993). Briefly, 1×10⁶ cells were washed with FACS medium and incubated on ice for 45 minutes with 100 µl of 100 µg/ml mAbs. The cells were then washed with cold FACS medium and reincubated with 100 µl of 20 µg/ml FITC-conjugated goat anti-rat IgG (H and L chains). After 45 minutes on ice, the cells were washed and analyzed by flow cytometry using a FACStar (Becton Dickinson, Mountain View, CA). Cells incubated with the second antibody alone served as control.

HA and CS binding assay

Lymphoma cells (1×10⁶) were incubated at 4°C with 20 µg/ml fluorescein-labeled HA (FL-HA) or 50 µg/ml fluorescein-labeled CS (FL-CS) in 100 µl FACS medium for 1 hour and analyzed by flow cytometry. The FL-HA and FL-CS were prepared as described (de Belder and Wik, 1975), except for FL-CS, where biotin-hydrazine was replaced by fluorescein hydrazide (Yang et al., 1995). The same cells incubated alone (autofluorescence) or with FL-HA or FL-CS and 1 mg/ml unlabeled HA or CS to competitively block ligand binding served as controls. To ascertain that the FL-HA and FL-CS binding was CD44-dependent, LB cells were also incubated with FL-HA or FL-CS in the presence of 100 µg/ml KM81 anti-CD44 mAb.

Shear assays on GAG-coated substrates

Cellular interactions on substrates coated with purified GAGs under shear flow were measured in a parallel-plate flow chamber as previously described (Lawrence et al., 1994; Clark et al., 1996). A polystyrene plate on which purified ligand had been adsorbed, was assembled in a parallel plate laminar flow chamber (260 µm gap) and mounted on the stage of an inverted phase-contrast microscope (Diaphot 300; Nikon, Japan). Hyaluronic acid (HA, 1 mg/ml or 0.5 mg/ml) or one of the other purified GAGs (1 mg/ml) was dissolved in PBS and adsorbed overnight at 4°C onto plastic petri dishes. The plates were blocked with 2% human serum albumin (Fraction V, Calbiochem, San Diego, CA) at 37°C for 2 hours. Flow was generated by an automated syringe pump (Harvard Apparatus, Natick, MA) attached to the outlet side of the flow chamber. Cultured cells were

washed twice with cation-free H/H medium (HBSS containing 10 mM Hepes, (pH 7.4) and 2 mg/ml BSA (Sigma, Fraction V)), concentrated to 10^6 cells/ml and perfused into the flow chamber at the desired shear stress for 60 seconds. Cellular interactions in several fields (1–4 fields of 0.17 mm^2 per data point) were videotaped and quantified directly from the monitor screen. Attachment of cells perfused under shear flow over an adhesive HA-coated substrate was considered stable if it was followed by rolling over a distance of at least 10 cell diameters or for at least 25 seconds. Detachment assays were performed using cells that had bound at stasis to ligand-coated plates for 30 seconds. After cell binding, wall shear stress was increased step-wise every 5 seconds (by a programmed set of flow rates delivered by the syringe pump) up to 15 dyn/cm^2 . At the end of each 5 second interval of increase in shear stress, the number of cells that remained bound relative to the number of cells that were attached at stasis was calculated. Background adhesive interactions of the cells with albumin-coated substrate were negligible, and essentially none of the transfectant cells remained bound to the control substrate above a shear stress of 0.1 dyn/cm^2 . The contribution of cells rolling into the observation field from upstream fields was minimized by locating the field at the upstream edge of the spot of adsorbed ligand. All assays were performed at room temperature (RT). For antibody blocking assays, 10^7 cells/ml were preincubated for 5 minutes at 4°C in binding medium with $100 \mu\text{g/ml}$ of different purified mAbs. The cells were diluted 1:10 in medium without washing out the antibodies and the suspension was perfused into the flow chamber. For inhibition with soluble GAGs, cells were suspended for 5 minutes at 24°C in binding medium in the presence of 1 mg/ml of the specified GAG and then perfused into the flow chamber. The GAG concentration was kept constant in the perfusate throughout the flow assay.

Co-precipitation of CD44 proteins with glycosaminoglycans by cetylpyridinium chloride

Cetylpyridinium chloride (CPC) precipitation (Scott, 1961; Lee et al., 1992) was used to analyze the binding of HA and other GAGs to the CD44 molecules of LB-TRv and LB-TRs cells. A quantity of 10^7 cells was washed three times in PBS, then lysed in cold PBS buffer containing 0.5% NP-40 and 1 mM phenylmethylsulfonyl fluoride (PMSF), and kept on ice for 30 minutes. The lysate was centrifuged at $10,000 \text{ g}$ for 10 minutes to remove insoluble material. Aliquots containing $100 \mu\text{l}$ of the lysate supernatant were mixed with $50 \mu\text{g}$ of HA, CS, heparin, HS or KS. After incubation for 1 hour at RT, $350 \mu\text{l}$ of 1.43% CPC were added to the samples and the suspensions were stirred and incubated at RT for 1 hour. The suspensions were then centrifuged (Eppendorf Inc., Fermtont, CA) at $10,600 \text{ g}$ for 10 minutes. After rinsing three times with 1% CPC containing 30 mM NaCl, the pellets were dissolved in $50 \mu\text{l}$ sample buffer (60 mM Tris-HCl, pH 6.8, 2% SDS, 10% glycerol, 0.01% bromphenol blue). After fractionation on SDS-PAGE (7.5% polyacrylamide) CD44s and CD44v proteins present in the pellet, were identified by western blot, using KM81 anti-CD44 mAb.

Assessment of local tumor growth and lymph node invasion

A quantity of 3×10^6 lymphoma cells was injected s.c. into the left flank, close to the hind limb of female BALB/c mice (5–8 mice per group). Development of the tumor at the injection site was monitored by recording tumor diameter (in cm) over time. To determine lymphoma invasion into the peripheral axillary and brachial lymph nodes, the organs were removed at various intervals following s.c. inoculation of the fluorescent tumor cells (GFP-expressing cell lines designated LB-G, LB-TRs-G, LB-TRv-G and LB-TRvM-G cells; G=green). Five mice were killed at each time point. The fluorescence of the lymph node was measured by a computerized FujiFilm Fluorescence Image Analyzer FLA-2000 (Fuji Photo Film, Japan), using an excitation wavelength of 473 nm and an emission wavelength of 520 nm . Quantitation of the fluorescence in the organ is expressed

as normalized emission intensity per area of the whole organ, using the following equation:

$$\left(\frac{\text{MFI of experimental lymph node}}{\text{size (cm}^2\text{) of experimental lymph node}} - \frac{\text{MFI of normal lymph node}}{\text{size (cm}^2\text{) of normal lymph node}} \right) \times \text{size of experimental lymph node} = \text{normalized MFI of experimental lymph node}$$

where MFI is the mean fluorescence intensity of the whole organ and the MFI of a normal lymph node is a measure of background autofluorescence.

To evaluate the effect of specific treatment with antibody or enzyme on local tumor growth or lymph node invasion, PBS, $150 \mu\text{g}$ IM7.8.1 anti-CD44 mAb, $150 \mu\text{g}$ 4D2 isotype matched control mAb, 20 units of hyaluronidase or 20 units of heparinase (similar specific activity) were injected into BALB/c mice. The intraperitoneal (i.p.) injections were started 6 days after s.c. tumor inoculation and continued every other day for 12 days (a total of 6 injections). Local tumor growth and lymph node invasion were evaluated as indicated above.

Immunofluorescence analysis of lymphoma cell accumulation and proliferation in lymph nodes

A quantity of 0.5×10^6 green lymphoma cells (LB-TRv-G, LB-TRvM-G, LB-TRs-G or LB-G cells) was injected intra-venously (i.v.) into BALB/c mice. The lymph node-infiltrating tumor cells were analyzed by three-color flow cytometry on different days post-injection, to simultaneously assess their representation among the lymph node cell population and the proportion of dividing cells among the infiltrating cells, as described (Kastan et al., 1991). Axillary lymph nodes were removed 4, 8 and 12 days post tumor injection and lymph node cells were incubated with 10^{-5} M BrdU for 30 minutes at 37°C in a CO_2 incubator. The cells were then harvested, fixed in cold 70% ethanol for 16 hours, and DNA was denatured in $2\text{N HCl}/0.5\%$ Triton X-100 (30 minutes, RT). To determine the percentage of GFP-expressing tumor cells in the lymph node, cells of high green fluorescence were gated. GFP-positive cells from each cell line were analyzed for BrdU staining and DNA content. Incorporation of BrdU was detected by staining with biotin-conjugated anti-BrdU antibody followed by CyTM5-conjugated streptavidin, and total DNA was stained with propidium iodide, $5 \mu\text{g/ml}$. The doubly treated cells were analyzed by flow cytometry, using a two laser FACSCaliber (Becton Dickinson). The percentage of BrdU-positive cells in the total GFP-positive population was recorded. This doubly fluorescent cell population represents dividing cells in the S-phase.

All the experiments described are representative of at least two, and in most cases, three trials all showing similar results.

RESULTS

LB T lymphoma cells transfected with CD44v4-v10 cDNA acquire the CD44-dependent ability to bind soluble HA and other GAGs

We previously suggested that mouse T-cell lymphoma (designated LB) dissemination is dependent on CD44-HA interaction, as injection of an anti-CD44 mAb directed against the constant epitope (pan-CD44) of the receptor, as well as injection of the enzyme hyaluronidase, reduced lymphoma invasion into the lymph nodes of BALB/c mice (Zahalka et al., 1995). We further reported that parental LB cells do not bind HA unless activated with phorbol ester (Vogt Sionov and Naor, 1997). Subsequently, it was found that HA binding to the activated cells is mediated by an upregulated CD44 variant,

whereas the standard CD44 of the same cells remains unoccupied by the ligand (Rochman et al., 2000). Similarly to PMA-activated LB cells, LB cells isolated from the peripheral lymph nodes, following their s.c. inoculation, exhibited an enriched repertoire of CD44 variants (Wallach et al., 2000), suggesting that they too represent a phase of activation. Collectively, those observations were the first indication that CD44v is important for both HA binding and HA-dependent tumor spread. This notion was substantiated by the subsequent experiments.

LB cells transfected with CD44v4-v10 (CD44v) cDNA were cultured in selective medium and cloned. Exon-specific RT-PCR analysis revealed that three representative clones of the transfected cells expressed the CD44v transcript (not shown). The total transfected cell population was designated LB-TRv. The individual clones were numbered (e.g. LB-TRv2, LB-TRv3). In parallel, LB cells were transfected with a control plasmid (designated LB-TRo) or with CD44s cDNA (designated LB-TRs) to overexpress this transcript. Parental LB cells, as well as LB-TRo, LB-TRs and LB-TRv cells, were analyzed for their ability to bind HA and other GAGs from the solution, to attach to GAGs under shear stress or to establish primary tumors and lymph node colonies *in vivo*.

LB cells, LB-TRs cells and six clones from two separate transfections (not shown), LB-TRv cells and two representative clones (TRv2 and TRv3) of six, from two separate transfections (Fig. 2A) or LB cells transfected with empty vector (LB-TRo cells; not shown), all expressed the CD44 constant epitope recognized by KM81 anti-pan CD44 mAb. By contrast, anti-CD44v4 and anti-CD44v6 mAbs stained only LB-TRv cells and their clones (Fig. 2A). The LB-TRv cells and their clones were also the only cells that bound FL-HA from the solution. Binding was blocked by an

excess of non-labeled HA (Fig. 2B), or by KM81 anti-CD44 mAb (Fig. 2C), but not by irrelevant isotype-matched control mAb (4D2; data not shown), proving that the interaction is CD44-dependent. Note that LB, LB-TRo and LB-TRv cells expressed the pan CD44 epitope to an almost equal extent. The LB-TRs cells, like LB and LB-TRo cells, neither expressed v4- and v6-encoded epitopes nor bound fluorescein-labeled HA, although they were the only cells that overexpressed CD44s (Fig. 2A). This finding supports the notion that the acquisition of the HA binding capacity by LB cells is related to the expression of CD44v-encoded epitopes rather than to overexpression of CD44 molecules. Flow cytometry analysis of parental LB cells as well as of LB-TRv cells and their clones, revealed that transfection of CD44v4-v10 cDNA into LB cells did not markedly influence the logarithmic expression of three different constant CD44 epitopes detected with anti-KM114, anti-IM7.8.1 and anti-KM81 mAbs, or of other cell surface adhesion molecules detected with anti-ICAM-1, anti-CD18, anti-CD11a and anti-CD11b mAbs (data not shown). In addition, none of the cell lines and clones expressed MEL-14.

To assess the ability of LB-TRv cells to bind CD44 ligands

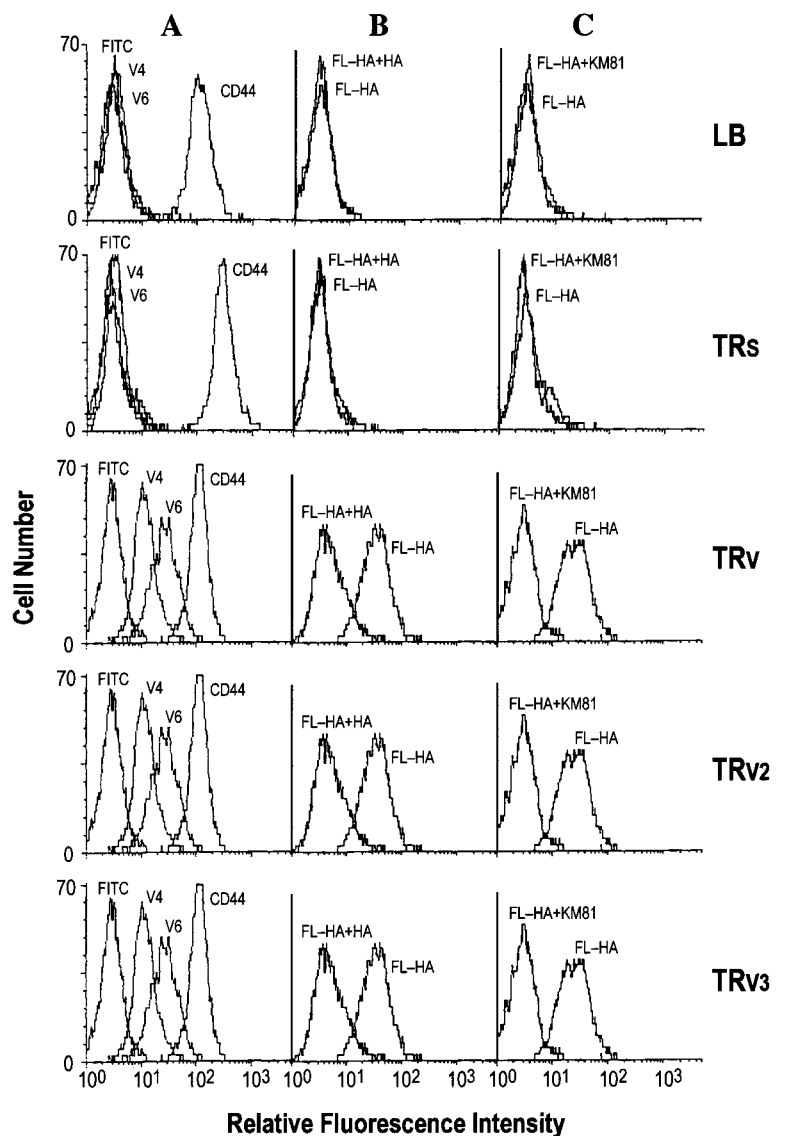
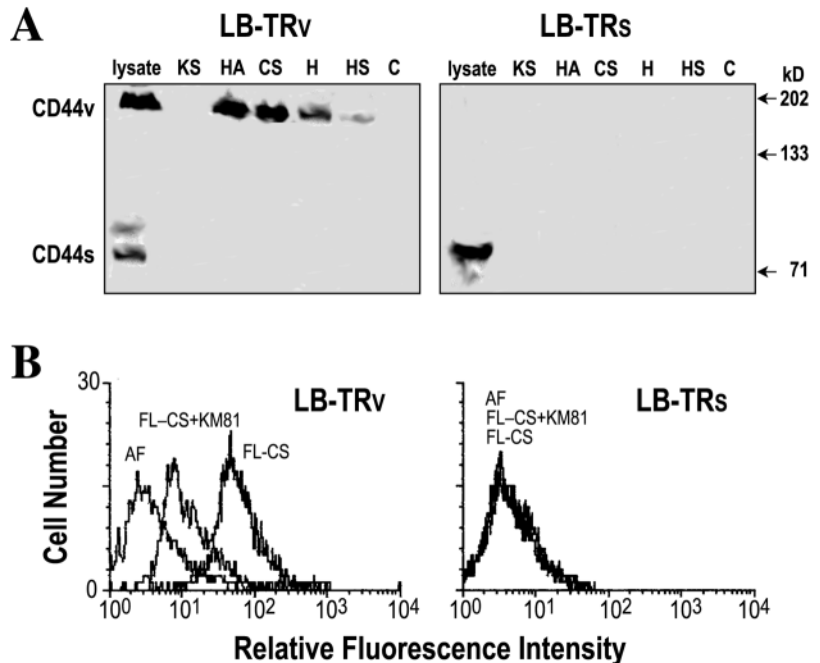


Fig. 2. LB cells transfected with CD44v4-v10 cDNA express v4 and v6-encoded epitopes and bind soluble HA. (A) Parental LB cells (LB), LB cells transfected with CD44s cDNA (TRs) as well as LB cells transfected with CD44v4-v10 cDNA (TRv) and two representative clones (TRv2 and TRv3) of six derived from two separate transfections, were analyzed by flow cytometry for CD44 isoform expression, as described in Materials and Methods. The cells were stained with KM81 anti-pan CD44 mAb (marked CD44), 10D1 anti-CD44v4 mAb (marked V4) and 9A4 anti-CD44v6 mAb (marked V6) followed by anti-rat IgG conjugated to FITC. FITC indicates cells stained with the second antibody alone. Note that the pan CD44 fluorescence intensity of the TRs cells is higher than that of the other cell lines. (B) LB, TRs and TRv cells, as well as representative TRv cloned cells, were incubated with fluorescein-labeled HA (20 μ g/ml) in the absence (FL-HA) or presence (FL-HA+HA) of unlabeled HA (1 mg/ml), which competitively inhibits the binding of FL-HA, and analyzed by flow cytometry. Segregated histograms display HA binding; matched histograms indicate the inability to bind HA. (C) All cells were incubated with fluorescein-labeled HA (20 μ g/ml) in the absence (FL-HA) or presence (FL-HA+KM81) of KM81 (IgG2b) anti-CD44 mAb (100 μ g/ml) and analyzed by flow cytometry. KM81 anti-CD44 mAb blocks the binding of FL-HA to TRv cells. The histograms of the LB-TRo cells were almost identical to those of the LB cells (not shown).

Fig. 3. Expression of a CD44 variant extends the ligand binding capacity of the lymphoma cells. (A) Western blots of CPC-precipitated CD44 derived from a total cell population of LB cells transfected with CD44v4-v10 cDNA (LB-TRv) or standard CD44 (LB-TRs). LB-TRv and LB-TRs cells were lysed and mixed with KS, HA, CS, H (Heparin) and HS. After CPC precipitation of GAG-associated proteins and their resolution on 7.5% SDS-PAGE (under nonreducing conditions), they were identified by western blot with KM81 anti-CD44 mAb. The last lane in each panel (marked by C) shows control precipitation (i.e. without the prior addition of GAGs). Lanes marked by 'lysate' show western blotting of the total cell lysate (no CPC precipitation) with anti-CD44 mAb. CD44v of LB-TRv cells binds HA as well as additional GAGs. (B) Flow cytometry analysis of CS binding to total LB-TRv and LB-TRs cell populations. LB-TRv and LB-TRs cells were stained with fluoresceinated CS (50 $\mu\text{g/ml}$) in the absence (FL-CS) or presence of KM81 anti-CD44 mAb (100 $\mu\text{g/ml}$) (FL-CS+KM81). Separate histograms display CS binding; matched histograms show the inability to bind CS. AF, autofluorescence.



other than HA, CPC analysis was performed (Scott, 1961; Lee et al., 1992). Cell lysates of LB-TRs and LB-TRv cells were incubated with HA or other GAGs (KS, HS, heparin and CS). As can be seen in Fig. 3A, HA, heparin, HS and CS, but not KS, caused CPC precipitation from LB-TRv cell lysates of a ~180 kDa CD44 variant isoform. All the GAGs, including hyaluronate, did not, however, cause precipitation of standard CD44 in lysates of LB-TRv cells, showing that CD44v, rather than CD44s, is involved in GAG binding. None of the GAGs interacted with the CD44 protein of the LB-TRs cell lysates. The binding of CS to LB-TRv cells, but not to LB-TRs cells, was confirmed by flow cytometry (Fig. 3B), using the fluorescein-labeled CS ligand. KM81 anti-CD44 mAb (Fig. 3B), but not irrelevant isotype-matched control mAb (4D2) as well as an excess of 1 mg/ml soluble CS (data not shown), blocked the binding, indicating that the CS binding is CD44-dependent.

LB cells transfected with CD44v4-v10 cDNA acquire CD44-adhesiveness to HA under shear stress flow

To determine if standard or variant CD44 expressed on LB transfectants mediate rolling adhesion on hyaluronate, the transfectants were temporarily settled on substrates coated with different GAGs, assembled in a flow chamber apparatus, and then subjected to increasing shear flow. LB-TRs, and in particular LB-TRv cells, established rolling adhesion and accumulated on HA-coated substrates (Fig. 4A). However, both transfectants failed to adhere, not even transiently, to control substrates coated with heparin, CS or KS (Fig. 4A). Accumulation of both CD44v and CD44s transfectants on immobilized HA was completely inhibited in the presence of function-blocking KM81 anti-CD44-mAb, but not in the presence of nonblocking KM114 anti-CD44 mAb or isotype-matched control mAb (Fig. 4B). Furthermore, soluble HA, but not CS and KS, efficiently impeded the ability of both LB-TRv (Fig. 4C) and LB-TRs (not shown) transfectants to establish rolling adhesion on immobilized HA.

We next compared the adhesive activity of the different CD44 isoforms in the context of shear flow, by perfusing the different cells on a given HA-coated substrate and quantifying the fraction of cells within each population capable of tethering and rolling on the immobilized CD44 ligand under various shear flow. The ability of the cells to tether to HA sharply decreased with increasing shear stress (Fig. 4D), as previously seen with other vascular receptors, including selectins and α 4 integrins (Springer, 1994; Alon et al., 1995; Berlin et al., 1995). Nevertheless, LB-TRv cells tethered and established rolling much more efficiently than did LB-TRs cells, in particular as the shear stress approached physiological levels (>1 dyn/cm²). At low shear stress (≤ 0.8 dyn/cm²) LB, LB-TRo and LB-TRs cells displayed appreciable rolling attachments, albeit less efficiently than LB-TRv cells (Fig. 4D,E). By contrast, LB-TRv cell rolling resisted detachment by elevated shear stress to a significantly greater extent than did LB, LB-TRo and LB-TRs cells (Fig. 4E; and data not shown). CD44 variant-expressing cells (LB-TRv) also rolled more slowly (3.54 ± 0.34 $\mu\text{m/sec}$) than the standard CD44-expressing cells (LB-TRs) (5.33 ± 0.39 $\mu\text{m/sec}$) at 2 dyn/cm². Collectively, all these differences were striking in light of the finding that the expression intensity of the total CD44 molecules (detected with KM81 anti-CD44 mAb) on LB-TRv cells was substantially lower than that on LB-TRs cells (Fig. 2). Thus, it can be concluded that a relatively small fraction of the CD44v isoform (i.e. CD44v4-v10) is capable of mediating tethering to and rolling on HA at physiological shear stresses.

A mutation in the HA-binding domain of cell surface CD44v inhibits its GAG binding capacity and interferes with its rolling attachments on HA substrate

The HA binding site of CD44v4-v10 was destroyed by replacing arginine with alanine at position 43 (analogous to position 41 in human CD44), and the construct was transfected into LB cells. The resulting transfectants, designated LB-

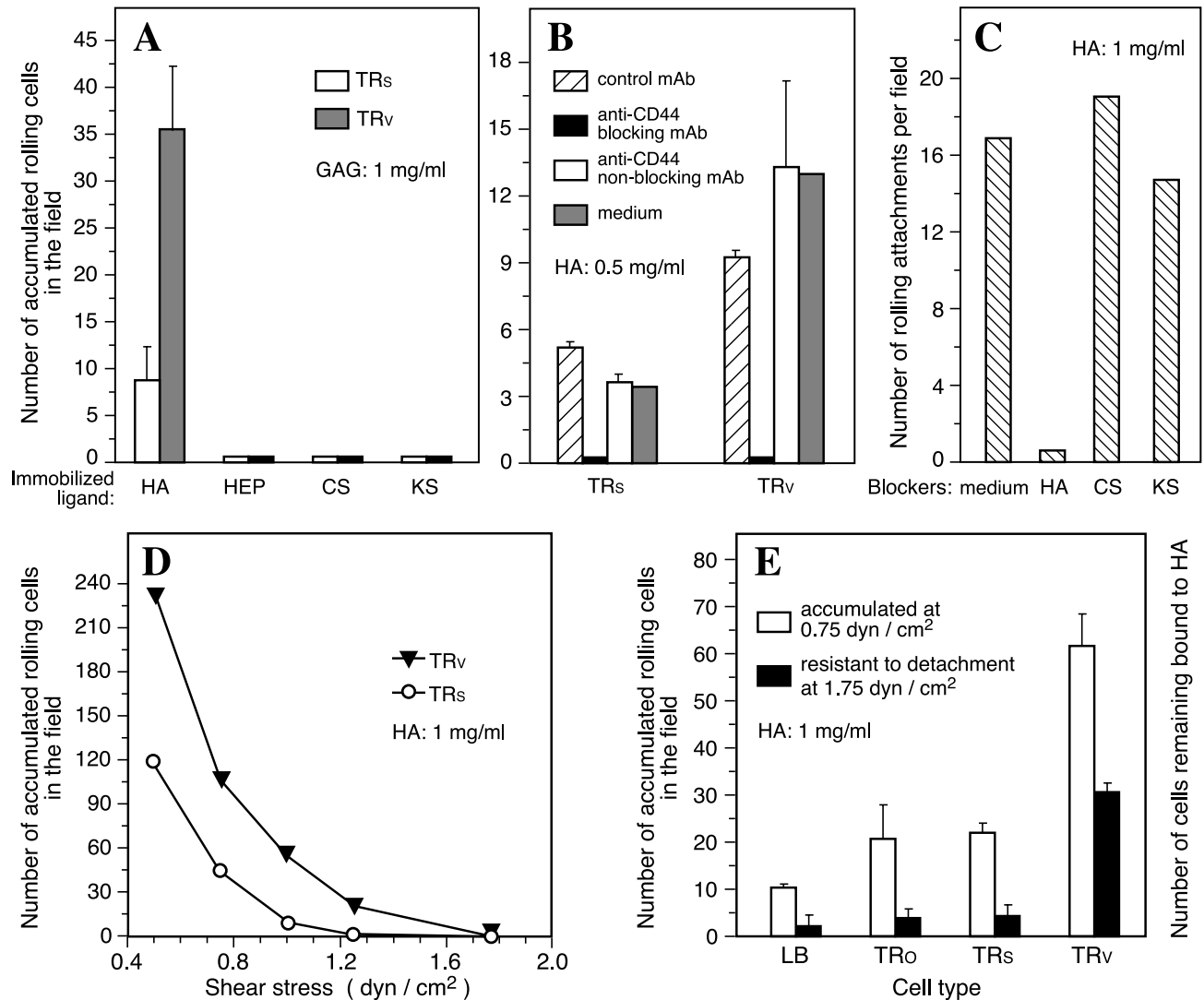


Fig. 4. Binding of LB cell line to HA under wall shear stress is mediated by CD44v. (A) Accumulation and rolling of LB-TRs and LB-TRv cells on different immobilized GAGs under shear flow. LB-TRs and LB-TRv lymphoma cells were allowed to settle for 100 seconds on different substrates, each coated with 1 mg/ml of a purified GAG, as indicated. The cells were subjected to a shear stress of 0.25 dyn/cm² for 5 seconds, followed by shear stresses of 0.5, 0.75 and 2 dyn/cm², each lasting for 5 seconds. The number of cells remaining attached at 2 dyn/cm² was counted at the end of the last interval of shear stress. (B) Effect of anti-CD44 mAbs on accumulation and rolling of CD44-transfected LB cells on HA. LB-TRv cells (10⁷ cells/ml) were pretreated with medium alone or with 100 µg/ml isotype-matched control mAb (4D2), blocking KM81 anti-CD44 mAb or nonblocking KM114 anti-CD44 mAb (5 minutes 4°C) in binding medium. The cells were diluted 1:10 with medium without washing out the antibodies and the suspension was then perfused into a flow chamber coated with 0.5 mg/ml HA. The cells were allowed to settle on the substrate and then subjected to increasing shear stress, as described in A. The number of cells remaining attached at 2 dyn/cm² was counted at the end of the last interval of shear stress. (C) Inhibition of attachment events (followed by rolling) of LB-TRv cells on immobilized HA with the following (1 mg/ml) soluble GAGs: HA, CS (chondroitin sulfate) and KS (keratan sulfate). Cells were perfused for 1 minute at a shear stress of 0.75 dyn/cm² over an HA (1 mg/ml) substrate. The number of cells that attached to and persistently rolled on the CD44 ligand was determined. (D) Effect of increasing shear stress on the rate of accumulation of CD44 transfectants on HA-coated substrate. LB-TRs or LB-TRv cells were perfused in multiple runs over a HA-coated field (1 mg/ml). Each perfusion run was performed at a different shear stress and lasted for 1 minute. The number of rolling cells accumulated at the end of each run is shown for each indicated shear stress. Note that at physiological shear stresses (>1 dyn/cm²), only LB-TRv cells were capable of persistent rolling on the HA field. (E) Accumulation and resistance to detachment of different lymphoma cell lines on HA. The indicated cells were accumulated for 1 minute at a low shear stress (0.75 dyn/cm²) and then subjected to a sharp increase in shear stress (1.75 dyn/cm²) for 20 seconds. The number of cells bound per field at the end of the accumulation period (marked accumulated) and after 20 seconds of high shear stress (marked resistant to detachment) are shown. The number of rolling cells was counted in one (C,D) or, if required, in two (A,B,E) representative fields. When two fields were counted, their mean ± range of determination are shown. All panels depict one of three independent experiments showing similar results.

TRvM, were cultured in selective medium and cloned. Flow cytometry analysis (Fig. 5A) revealed that, in comparison with LB-TRv cells, the total cell population of LB-TRvM cells, as

well as six clones of two separate transfections (not shown), all expressing the mutated CD44v, lost their ability to bind soluble HA (Fig. 5A, right panels), whereas the level of their

CD44 (pan and v6) (Fig. 5A, left panels) and CD18 adhesive proteins (not shown) remained unchanged. Also, CPC analysis (not shown) showed that LB-TRvM cells bound neither HA nor other GAGs (heparin, HS, CS and KS). The inability to bind CS by LB-TRvM cells was confirmed by flow cytometry (Fig. 5B). Furthermore, the mutated CD44v4-v10 isoform expressed in LB-TRvM cells did not exhibit any attachment and rolling capacity above the corresponding endogenous activities of the standard isoform expressed in LB-TRs cells (Fig. 4D), as shown under both physiological and hyperphysiological shear stress (data not shown).

LB cells transfected with CD44v4-v10 cDNA, but not with the corresponding non-HA binding mutant, display enhanced growth in BALB/c mice

LB-TRv cells, in contrast to LB-TRs cells or the parental LB cells, interact with soluble HA and display rolling attachments on HA substrate under physiological shear stress (Fig. 2; Fig. 4). If the *in vitro* migratory advantage of LB-TRv cells is also reflected *in vivo*, we should expect to find that LB-TRv cells disseminate more efficiently than LB-TRs cells or parental LB cells. To allow the detection of disseminated lymphoma cells following their *s.c.* inoculation into BALB/c mice, all cells lines were transfected with a GFP expression vector. Localization of the green tumor cells in the lymphoid organs was quantified by normalizing the intensity of organ fluorescence according to organ size (as described in Materials and Methods). Fig. 6A shows that the fluorescent (green) LB-TRv cell line (TRv-G), developed local tumors faster than did the green LB-TRs (TRs-G) and LB (LB-G) cells following *s.c.* inoculation of 3×10^6 cells. Also, *s.c.* inoculated LB-TRv-G cells invaded the peripheral lymph nodes more rapidly than did LB-G and LB-TRs-G cells, as indicated by the normalized MFI of the whole lymph node (Fig. 6B). As can be seen, the tumors with the highest cell rolling capacity also exhibited faster growth and invasion.

LB cells transfected with CD44v4-v10 mutated at the HA binding site (LB-TRvM cells), were unable to bind soluble HA from the solution, and failed to roll on HA substrate under physiological shear stress. Therefore, we examined whether the mutated HA binding site of LB-TRvM cells influences their ability to accumulate in the lymph nodes of BALB/c mice. Fig. 6C shows that the green LB (LB-G) and LB-TRvM (expressing the mutated CD44) (LB-TRvM-G) cells displayed markedly slower local tumor growth than did the green LB-TRv (LB-TRv-G) cells following *s.c.* inoculation. In addition, the green LB-TRvM cells (LB-TRvM-G), in contrast to the green LB-TRv

cells (LB-TRv-G), did not invade the peripheral lymph nodes to any considerable extent, as indicated by measuring the normalized mean fluorescence intensity of the whole organ (Fig. 6D).

Cell lines and clones of nonfluoresceinated LB-TRv, LB-TRs and LB-TRvM, displayed local tumor development and lymph node invasion (8 mice in each group) that were only slightly faster (but statistically significant) than those of the corresponding fluoresceinated cells (derived from separate CD44 transfections) (data not shown), thereby confirming the growth advantage of cells expressing CD44v.

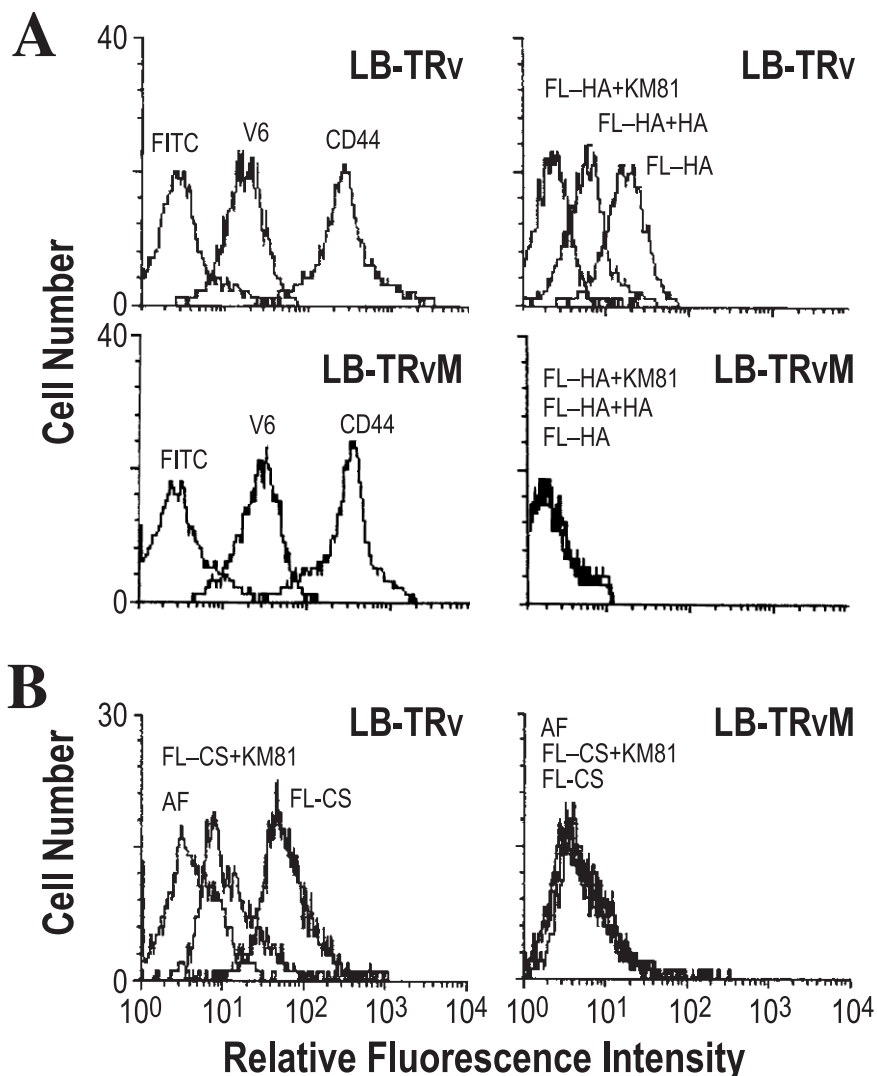
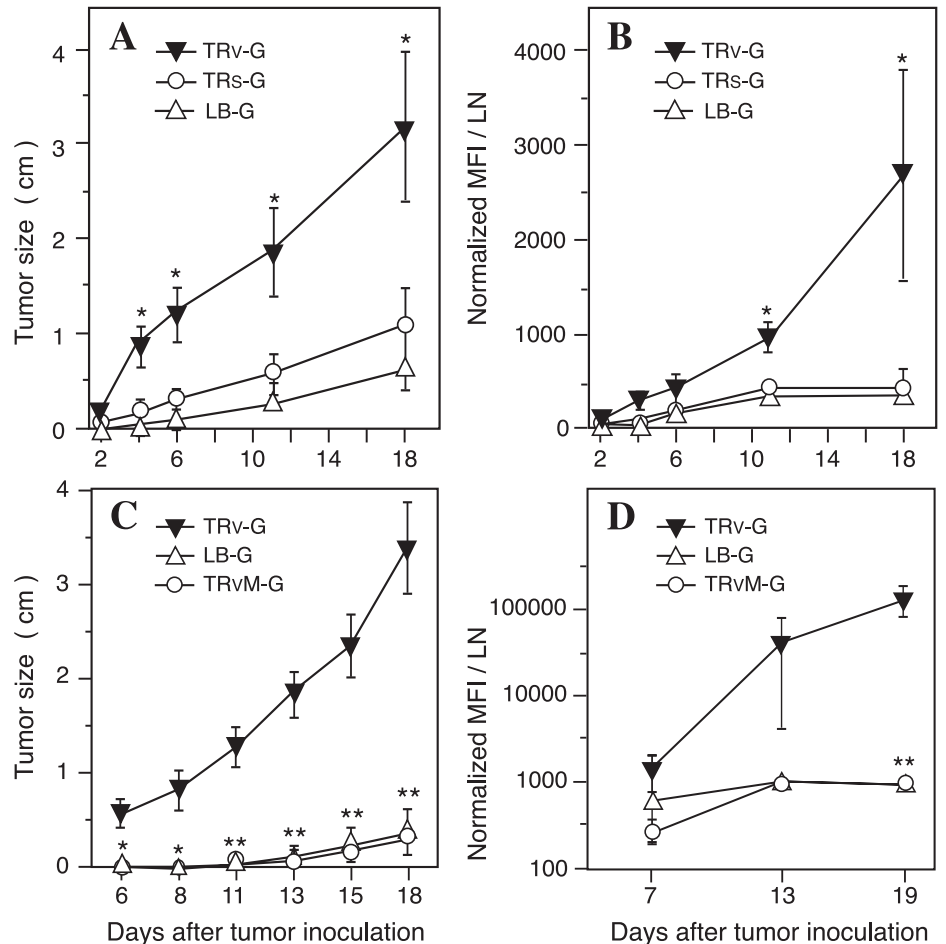


Fig. 5. LB cells transfected with CD44v4-v10 cDNA mutated at the HA binding site lose their ability to bind HA and CS. (A) LB cells transfected with CD44v4-v10 cDNA (LB-TRv) (top panels) and LB cells transfected with CD44v4-v10 cDNA mutated at the HA binding site (LB-TRvM) (bottom panels) were indirectly analyzed by flow cytometry for expression of CD44 isoforms (pan CD44 and v6; left panels), as described in the legend to Fig. 2. In addition, the cells (right panels) were incubated with fluorescein-labeled HA (20 $\mu\text{g}/\text{ml}$) in the absence (FL-HA) or presence of unlabeled HA (1 mg/ml) (FI-HA+HA) or KM81 anti-CD44 mAb (100 $\mu\text{g}/\text{ml}$) (FI-HA+KM81) and analyzed by flow cytometry. Segregated histograms display HA binding; matched histograms indicate the inability to bind HA. (B) LB-TRv and LB-TRvM cell lines were subjected to flow cytometry to test their ability to bind FL-CS, as described in the legend to Fig. 3. LB-TRvM cells did not bind CS. AF, autofluorescence.

Fig. 6. LB cells transfected with CD44v4-v10 cDNA show more efficient local tumor formation and lymph node accumulation than LB cells transfected with standard CD44 cDNA or LB cells transfected with mutated CD44v4-v10 cDNA. Green fluorescent protein (GFP) cDNA was transfected into LB-TRv (TRv-G), LB-TRs (TRs-G) (both derived from independent CD44 transfections different from those of the corresponding nonfluoresceinated lymphoma cells) and parental LB (LB-G) cells. A quantity of 3×10^6 cells from each transfected cell population was s.c. injected into BALB/c mice. The size of the local tumor (\pm s.e.m.) at the injection site (A) was measured at different time points after tumor inoculation (5 mice from each group were killed at each time point). Invasion of a peripheral lymph node (B) by the green lymphoma cells at different time points after tumor inoculation is indicated by the normalized mean (\pm s.e.m.) fluorescence intensity (MFI) of the whole organ (5 animals from each group were tested for lymph node invasion at each time point). In another experiment, BALB/c mice were s.c. inoculated with 3×10^6 green LB cells transfected with mutated CD44v4-v10 cDNA (TRvM-G), green LB cells transfected with wild-type CD44v4-v10 cDNA (TRv-G) or green parental LB cells (LB-G). At each time point, 5 mice from each group were killed. Local tumor size (C) (\pm s.e.m.) and the intensity of lymph node invasion (D) (\pm s.e.m.) were assessed at different time points after tumor inoculation. * $P < 0.05$; ** $P < 0.01$ by Mann-Whitney, compared with LB-G (A,B) or TRv-G (C,D). Note that the asterisks in C and D mark the two lines (LB-G, TRvM-G).



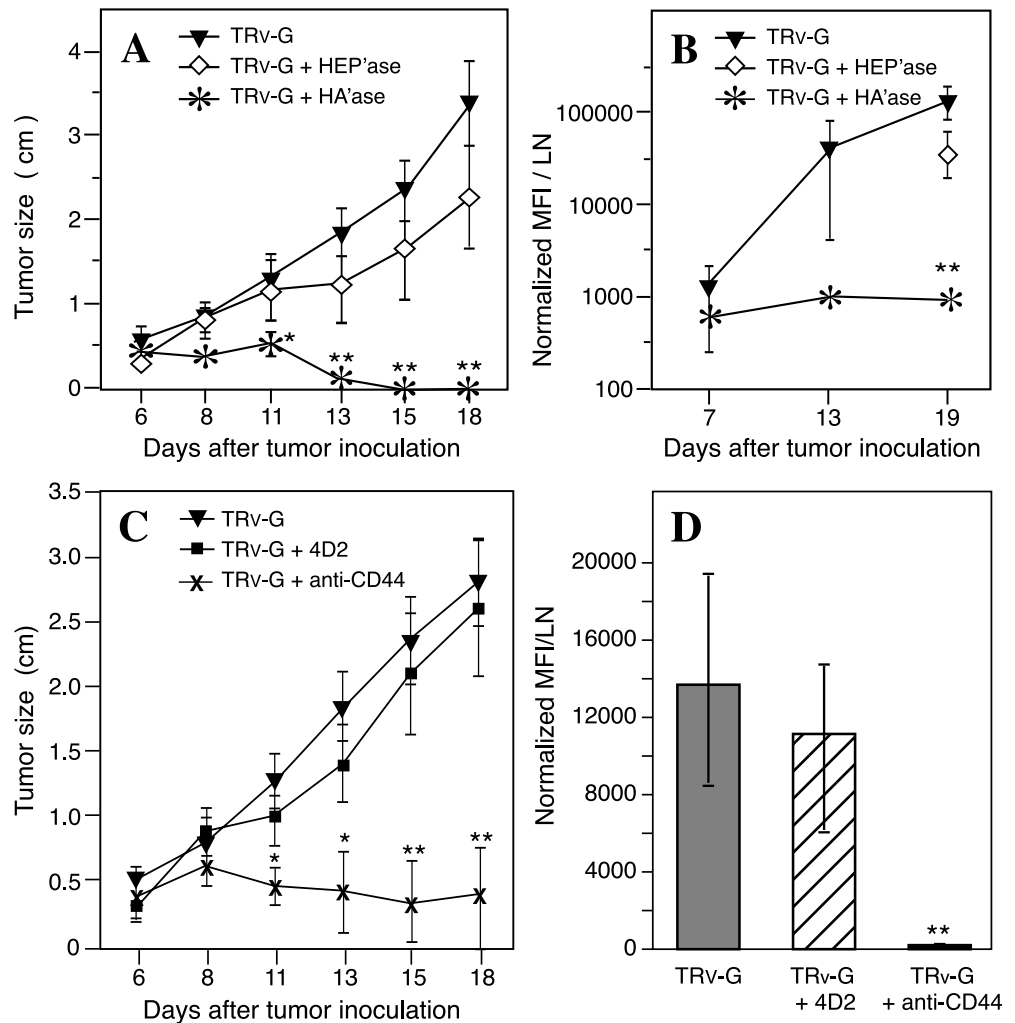
The above findings are supported by a subsequent experiment in which systemic injection of hyaluronidase 6 days after fluorescent LB-TRv lymphoma s.c. inoculation and then every other day for 12 days, markedly reduced local development of the tumor (Fig. 7A) and lymph node invasion (Fig. 7B). Administration of heparinase of the same specific activity, following an identical protocol, influenced neither local tumor growth nor lymph node invasion (Fig. 7A,B). In addition, injection of IM7.8.1 anti-CD44 mAb, but not of isotype-matched control mAb (4D2; to exclude Fc-mediated killing), adhering to the protocol used for enzyme treatment, suppressed local development of fluorescent LB-TRv cells (Fig. 7C) and their invasion of the lymph nodes (Fig. 7D). Note that IM7.8.1 anti-CD44 mAb interferes with HA binding to activated LB lymphoma cells (Vogt Sionov and Naor, 1997).

Enhanced accumulation of LB-TRv cells in peripheral lymph nodes is a result of intensive migration of the lymphoma cells

Subcutaneously inoculated LB-TRv cells accumulated in the lymph nodes more rapidly than did LB-TRv cells mutated at the HA binding site (LB-TRvM cells), LB-TRs cells or parental LB-cells (Fig. 6). The enhanced accumulation of LB-TRv cells in the peripheral lymph nodes may be attributable to

efficient cell migration or to extensive cell division. Analysis of the division rate of the different lymph node-infiltrating tumor cells should help to resolve this issue. To circumvent cell release from the primary tumor growth, GFP-expressing lymphoma cells were injected intravenously. Fig. 8 shows flow cytometric analysis of peripheral lymph nodes removed on days 4, 8 and 12 from BALB/c mice, following i.v. administration of GFP-expressing LB-TRv, LB-TRvM, LB-TRs and LB cells. The proportion of green LB-TRv cells in the lymph node cell suspension was markedly higher than that of the other lymphoma cell types (A in each box of Fig. 8), indicating their enhanced accumulation in the lymphoid organ as a function of time (i.e. independent confirmation of the results described in Fig. 6). To determine the proliferation rate of the GFP-lymphoma cells in the lymph nodes, BrdU incorporation into replicating DNA versus total DNA content were analyzed by flow cytometry, using anti-BrdU antibody and propidium iodide, respectively. A comparison of GFP-positive cells from each cell line (Fig. 8; detailed results are represented for day 12 only) revealed that all types of tumor cells (including LB-TRv cells) displayed a similar proportion of cells in the S-phase (B in each box of Fig. 8). This finding implies that the enhanced accumulation of LB-TRv cells in the lymph nodes is attributable to efficient migration into the

Fig. 7. The effect of hyaluronidase and anti-CD44 mAb on local tumor growth and lymph node invasion by LB-TRv lymphoma cells. BALB/c mice were s.c. inoculated with 3×10^6 green LB-TRv cells (TRv-G). After 6 days, PBS (TRv-G), 20 units heparinase (TRv-G + HEP'ase) or hyaluronidase (TRv-G + HA'ase) of equivalent specific activity was injected i.p. into the mice (A,B). Using the same injection protocol, but in a different experiment, other groups of mice received PBS (TRv-G), isotype-matched control mAb (TRv-G+4D2) or IM7.8.1 anti-CD44 mAb (TRv-G+anti-CD44) (C,D). PBS, enzymes and antibodies, were injected every other day for 12 days (a total of 6 injections). Five mice from each group were killed at each time point. Local tumor size (A,C) and the intensity of lymph node invasion (B,D) were assessed at different time points, as described in Fig. 6. Statistical analysis as indicated in Fig. 6; all groups were compared with the TRv-G group. Note that the intensity of lymph node invasion following heparinase (B) or antibody injection (D) was assayed on day 19 only.



lymph node rather than to accelerated cell division inside it. Using two-color flow cytometry analysis (staining with anti-BrdU antibody and propidium iodide) to determine the basal proliferation rate of LB, LB-TRv, LB-TRs and LB-TRo cells, we found that their proportion in the S-phase was similar (i.e. 32.08, 24.88, 32.06 and 30.87%, respectively).

DISCUSSION

Our findings show that LB lymphoma cells transfected with CD44v4-v10 cDNA (LB-TRv cells), but not corresponding cells transfected with CD44s cDNA (LB-TRs), to overexpress the endogenous CD44s, acquire a strong HA binding capacity both in solution and under dynamic flow conditions. Moreover, enhanced local tumor formation and tumor accumulation in lymph nodes were observed following s.c. inoculation of the CD44v (but not CD44s)-transfected cells into BALB/c mice. LB cells transfected with empty vector and parental LB cells behaved like LB-TRs cells with respect to the above mentioned experimental parameters. Moreover, LB cells transfected with CD44v4-v10 cDNA subjected to a single mutation at the HA binding site (LB-TRvM cells) lost their increased ability to interact in solution or under shear stress with HA and to develop lymph node tumors following s.c. inoculation. Hence,

the addition of the variant sequence in the membrane proximal region of the CD44 receptor may directly confer the HA binding function. Alternatively, it may indirectly influence the HA binding capacity of the distal N-terminus site in the constant domain of the same molecule due to post-translational modifications that are unique to the variant exons. Although this issue has not been resolved, these data advocate (1) CD44v (not CD44s)-associated binding to HA in solution; (2) the increased ability of cell surface CD44v to support rolling attachment on immobilized HA under physiological shear stress; and (3) CD44v-associated tumor formation and lymph node invasion, which appear to be dependent on the interaction with HA. Although we are aware of the possibility of clonal variation, we believe that the identical behavior of the total cell population and several independent clones derived from two separate transfections supports our conclusion.

Since the establishment of metastatic colonies in secondary organs may be dependent on the trafficking potential of the cancer cells, we focused our attention on the cell motility of LB cells. Our results show that CD44v, rather than CD44s, can provide the dynamic reversible bonds required for the interaction between migrating cells and their substrate (Duband et al., 1988). The finding that LB-TRv cells display CD44-dependent binding to HA under flow stress and roll under physiological shear stress, suggests that the CD44v-

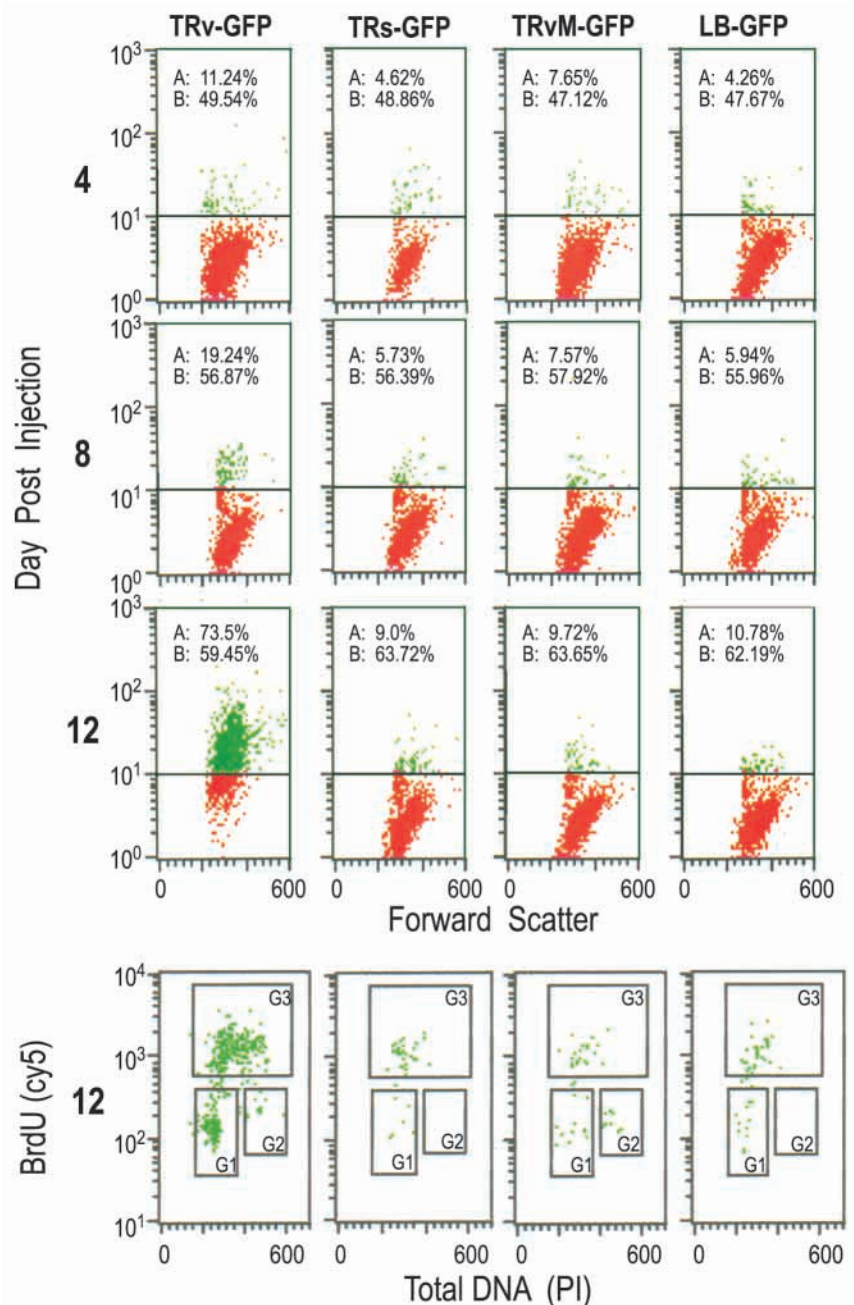
ligand pair rapidly establishes bonds that are sufficiently strong to maintain provisional cellular contacts with the substratum, but not strong enough to cause permanent cell arrest (Lauffenburger, 1991; DiMilla et al., 1993). However, these cellular contacts can be established by the interaction of CD44v with immobilized HA, but not with other immobilized GAGs (Fig. 4A). CD44v binding to non-HA GAGs is presumably not sufficiently strong to resist cell detachment from the substratum under physiological fluid shear stress.

LB-TRs and parental LB cells displayed weak rolling attachments on HA substrate under low shear stress (0.2-0.8 dyn/cm²), but failed to bind HA from the solution (Fig. 2). This dichotomy was also observed in certain cells whose cytoplasmic tail-truncated CD44 does not bind soluble HA, although it is still able to interact with immobilized HA (Lesley et al., 1992). These findings prove that under low shear stress (0.2-0.8 dyn/cm²), immobilized HA can weakly interact with cell surface CD44s, possibly due to its ability to crosslink cell surface receptors. This no longer holds true, however, when the shear stress approaches physiological levels. Under such conditions, only LB cells expressing CD44v can accumulate and roll on HA, possibly due to its ability to undergo oligomerization upon interacting with the multivalent HA ligand (Sleeman et al., 1996a). The oligomerization of CD44v may lead to the coalescence of the microdomains (Ilanguvaran et al., 1999), resulting in the redirection of cytoskeleton actin bundles, which are associated

with the microdomains in the cytoplasmic leaflets (Oliferenko et al., 1999). If this is the case, the association of CD44v, rather than of CD44s, with the detergent-resistant complexes in raft domains may explain how this isoform mediates HA-dependent rolling in LB-TRv cells.

Using a parallel plate flow chamber simulating physiological shear stress, it was previously demonstrated that the CD44 receptor can support HA-dependent rolling attachments (primary adhesion) of lymphoid cell lines (both activated and nonactivated) and of primary activated lymphocytes (DeGrendele et al., 1996; DeGrendele et al., 1997b; Mohamadzadeh et al., 1998), tonsillar lymphocytes (Clark et al., 1996; Estess et al., 1998), lymphocytes from patients with autoimmune diseases (Estess et al., 1998) and lymphoma cells (Clark et al., 1996). It is clear that in at least some cell types,

Fig. 8. Accumulation and proliferation of lymphoma cells in the peripheral lymph nodes following i.v. injection. The indicated fluorescent lymphoma cells were injected i.v. into BALB/c mice. Three-color flow cytometric analysis of their lymph node cell suspensions was performed on days 4, 8 and 12 postinjection to show the accumulation of the different lymphoma cell lines as a function of time. The upper edge of the autofluorescence spot of normal lymph node cells (not shown) was used to determine the horizontal line bordering the lymph node cells (below the line) and the green tumor infiltrating cells (above the line). The percentage of GFP-positive infiltrating tumor cells (above the line; A in each box) in the total lymph node cell suspension (the sum of cells below and above the horizontal line (i.e. 7000 events) was determined by plotting green-fluorescence intensity (on a logarithmic scale) versus forward scatter. The green lymphoma cells (above the horizontal line) were gated and the proportion of BrdU-labeled dividing cells in the S-phase (B in each box) was determined following staining with anti-BrdU antibody and propidium iodide, as indicated in Materials and Methods. The percentage of cells in the S-phase (shown for day 12) was determined by dividing the number of cells framed in G3 by the total cell number (G1+G2+G3) × 100. A similar formula was used to calculate the proportion (percentage) of cells in the S-phase at days 4 and 8. Note that the proportion of dividing cells in the population of green cells (i.e. lymphoma cells) is similar in all four cell lines, indicating a similar proliferation rate.



such as the BW5147 cell line (DeGrendele et al., 1996), CD44s is involved in the cell rolling attachments under physiological shear, as in this cell line only the standard form of CD44 is expressed (Trowbridge et al., 1982; DeGrendele et al., 1997b). By contrast, we now show, for the first time, that cell surface CD44v (CD44v4-v10), rather than CD44s, is involved in LB lymphoma rolling attachment on HA substrate under physiological shear stress. It seems unlikely that integrins play an independent or mandatory role in the dynamic CD44-mediated binding of the LB lymphoma to HA substrate, as the level of these molecules on LB-TRv and LB-TRs cells is almost identical, yet only the former display efficient rolling. Selectins are definitely not involved in the rolling process on HA, as LB cells are deficient in these molecules, and also because rolling was independent of Ca^{2+} , which is required for selectin function.

These *in vitro* rolling studies are matched by their *in vivo* counterparts. LB-TRv cells form local tumors and accumulate in the peripheral lymph nodes much more rapidly than do parental LB cells and LB-TRs cells. Furthermore, both the rolling of LB-TRv cells on HA substrate *in vitro* and lymph node accumulation of LB-TRv cells *in vivo* are dependent on the CD44-HA interaction, as these events are disrupted in LB-TRv cells expressing CD44v mutated at the HA binding site. These conclusions are supported by the observation that LB-TRv cells treated with anti-CD44 mAb (both *in vitro* and *in vivo*), an excess of soluble HA (*in vitro*), or the enzyme hyaluronidase (*in vivo*) lost their ability to roll on HA substrate *in vitro* and to form aggressive tumors *in vivo*. These correlated *in vitro* and *in vivo* findings suggest that a similar mechanism supports the migration of LB-TRv cells both in the flow chamber and in the intact animal. If this assumption is correct, the enhanced accumulation of LB-TRv cells in the peripheral lymph nodes, when compared with that of LB and LB-TRs cells, should be the result of their efficient migratory capacity rather than of intensive local proliferation in the invaded organ. In agreement with this premise, it was found that the proliferation rate of LB-TRv cells in culture and in the lymph nodes *ex vivo* (following *i.v.* injection) is similar to that of LB, LB-TRvM and LB-TRs cells, while the absolute number of LB-TRv cells detected in the same organ is far larger than that of the other cell lines. These findings suggest that cell surface CD44v supports efficient migration of the tumor cells into the lymph nodes, possibly following their previous localization in the lung or spleen. This could be the result of faster and/or more efficient migration (as shown *in vitro* in the flow chamber) or of larger numbers of migrating cells entering the lymph nodes, events that are sensitive to anti-CD44 mAb and hyaluronidase. The alternative explanation that LB-TRv cells proliferate at higher rates than the other cell lines, due to their preferential stimulation by lymph node-localized HA or growth factors, does not reconcile with the data of Fig. 8, which shows a similar proliferation rate for all the cell lines, despite the fact that LB-TRv cells exhibited faster accumulation. Furthermore, since LB-TRv cells were transfected with CD44v4-v10 cDNA, they do not express v3, an exon product known to bind HS-recognizing growth factors (Bennett et al., 1995; Jones et al., 2000). Hence, such factors are not involved in the stimulation of these tumor cells.

Note that the number of TRv-GFP cells from day 4 to day 12 increased by 6.5-fold (as percent cells in the lymph node), whereas the rest of the cell lines increased by 1.3 (TRvM-GFP

cells) to 2.5-fold at that time. Taking into account that about 50-60% of all cell types are engaged in division, the number of cells (including the number of TRv-GFP cells) at day 12 would be expected to be higher. This phenomenon can be explained by the high death rate of cells accumulating in the lymph node as well as by the differential selective death between TRv-GFP cells and TRvM-GFP cells or the other cell lines. Our findings do not exclude accelerated proliferation of LB-TRv cells in the primary tumor growth (or in intermediate organs) and the consequent intensive release of mobile cells that migrate into the lymph nodes. However, to allow direct analysis of tumor cell accumulation in the lymph nodes, the various cell lines were injected intravenously rather than subcutaneously.

How can we explain the ability of anti-CD44 mAb or hyaluronidase to reduce local tumor growth and tumor accumulation in the lymph node when injected six days after lymphoma inoculation (Fig. 7)? At this point in time, inhibition of tumor migration by these agents can not explain the reduced tumor growth and we must, therefore, seek an alternative interpretation. It has been previously reported that interference with integrin- (Meredith and Schwartz, 1997) or CD44- (Tian et al., 2000) dependent cell attachment to substrate (e.g. by antibody) activates the signaling of programmed cell death. A similar mechanism of apoptosis may be valid after injection of anti-CD44 mAb or hyaluronidase into mice bearing LB lymphoma, as both agents could disrupt the tumor-substrate interaction in the primary growth and secondary organs, an interaction essential to adhesion-dependent survival. Consequently, the tumor cell reservoir in the local growth may be reduced and a smaller number of cells released and seeded in the lymph nodes. While this notion is not necessarily incompatible with the interpretation that anti-CD44 or hyaluronidase also interferes with tumor cell migration from the local growth to the lymph nodes, it provides a possible explanation for the failure of all cell lines other than TRvG cells to grow efficiently in the nodes following *i.v.* injection (Fig. 8). According, we suggest that most of the lymph node-infiltrating lymphoma cells that do not express an efficient HA-binding CD44 receptor, fail to interact with the substrate and undergo a process of apoptosis. Some of these cells survive and proliferate, perhaps due to their ability to attach to the ECM via integrins or other cell surface adhesion receptors. By contrast, LB-TRv cells have a relative survival advantage in the lymph node environment as they are the only cells that can establish efficient contacts with ECM via the CD44-HA interaction and, therefore, initiate DNA synthesis.

Although the suggestion that anti-CD44 mAb or hyaluronidase interferes with LB-TRv cell migration is based mostly on the correlation with the *in vitro* rolling studies, it clearly points to the significance of the CD44-HA interaction in lymphoma spread and to the practical implications of the finding (i.e. the potential use of CD44 or HA as therapeutic targets).

We suggest that the CD44-HA interaction is essential to lymph node invasion by the lymphoma cells. In this context, it should be noted that the lymph nodes and their afferent lymphatics contain hyaluronate (Fraser and Laurent, 1989; Aruffo et al., 1990), which may support the penetration of the tumor cells into these organs via the afferent lymphatics, as shown by us previously (Zahalka et al., 1995). Furthermore, as

LB-TRv cells are deficient in L-selectin (Mel-14) they cannot enter the lymph nodes via the high endothelial venule (HEV) (Springer, 1994).

We previously showed that the HA9 cell line, a variant selected from the LB cell population by multiple cycles of binding to HA substrate, displayed enhanced expression of v4 and v6 CD44 epitopes and constitutively bound HA (Vogt Sionov and Naor, 1997). But, unlike LB-TRv cells, this cell line showed a reduced capacity to invade the lymph nodes when compared with the parental LB cells. Quantitative and/or qualitative differences in CD44 isoform expression may explain why the disseminational behavior of the tumors is at variance.

We would like to avoid generalizations at this time since the relationship between HA binding and tumor properties seems to be complex. For instance, in a pancreatic carcinoma model, CD44v expression was correlated with HA binding (Sleeman et al., 1996b) and metastatic behavior (Günther et al., 1991). However, hyaluronidase overexpression on the surface of these cells, which efficiently abolished any interaction with HA, did not alter their metastatic potency (Sleeman et al., 1996b). In human lymphoma and melanoma, HA binding was correlated with CD44s, not CD44v, overexpression (Sy et al., 1991; Bartolazzi et al., 1994; Bartolazzi et al., 1995) and tumor growth in vivo was supported by cell surface CD44s, but not by an HA-nonbinding CD44s mutant (Bartolazzi et al., 1994). As the human and mouse CD44 variable region shows only partial homology (65%; Screaton et al., 1993), we suggest that its influence on the functional behavior of the entire molecule (including HA binding and the support of tumor progression) differs in the two species. However, because CD44 displays contradictory molecular functions, we need to know more about the mechanisms of CD44 action before venturing any further interpretation of these findings.

The same caution is warranted in evaluating the clinical data. Attempts to correlate cell surface expression of CD44 in general and CD44v in particular with the malignant status of human tumors have yielded conflicting results (Naor et al., 1997). Nevertheless, there is well-documented data on many human malignancies (e.g. renal epithelial cancer (de Alava et al., 1998), papillary thyroid carcinoma (Kurozumi et al., 1998), vulvar cancer (Tempfer et al., 1998), pancreatic cancer (Rall and Rustgi, 1995) and non-Hodgkin's lymphomas (Salles et al., 1993; Stauder et al., 1995)), showing that the more progressive or metastatic phenotypes express v6-containing CD44 isoforms (Naor et al., 1997).

Furthermore, we believe that this report makes a significant contribution to our understanding of cell migration in malignant diseases and perhaps in other diseases whose pathology is cell trafficking-dependent (as shown by us for inflammatory cell migration in insulin-dependent diabetes; Weiss et al., 2000). It has been shown in an in vitro assay that the LB lymphoma uses CD44v for the rolling interaction with HA substrate. This activity may mimic in vivo adhesive and migratory cellular processes on the HA of the vasculature and ECM, essential to lymphoma dissemination. Furthermore, at a given level of expression, CD44v confers on LB cells three properties: GAG binding, rolling under physiological shear forces and enhanced accumulation in the lymph nodes. This strongly suggests that one and the same molecule is responsible for similar effects both in vitro and in vivo.

We thank Gila Neiman for her assistance in FACS cell sorting, Alexandra Mahler for her editorial assistance and Sharon Saunders for typing the manuscript. This work was supported by the German-Israeli Foundation for Scientific Research and Development (GIF) and a grant from the Deutsche Krebshilfe, Mildred Scheel Stiftung.

REFERENCES

- Alon, R., Kassner, P. D., Carr, M. W., Finger, E. B., Hemler, M. E. and Springer, T. A. (1995). The integrin VLA-4 supports tethering and rolling in flow on VCAM-1. *J. Cell Biol.* **128**, 1243-1253.
- Aruffo, A., Stamenkovic, I., Melnick, M., Underhill, C. B. and Seed, B. (1990). CD44 is the principal cell surface receptor for hyaluronate. *Cell* **61**, 1303-1313.
- Bartolazzi, A., Peach, R., Aruffo, A. and Stamenkovic, I. (1994). Interaction between CD44 and hyaluronate is directly implicated in the regulation of tumor development. *J. Exp. Med.* **180**, 53-66.
- Bartolazzi, A., Jackson, D., Bennett, K., Aruffo, A., Dickinson, R., Shields, J., Whittle, N. and Stamenkovic, I. (1995). Regulation of growth and dissemination of a human lymphoma by CD44 splice variants. *J. Cell Sci.* **108**, 1723-1733.
- Bennett, K. L., Jackson, D. G., Simon, J. C., Tanczos, E., Peach, R., Modrell, B., Stamenkovic, I., Plowman, G. and Aruffo, A. (1995). CD44 isoforms containing exon v3 are responsible for the presentation of heparin-binding growth factor. *J. Cell Biol.* **128**, 687-698.
- Berlin, C., Bargatze, R. F., von Andrian, U. H., Szabo, M. C., Hasslen, S. R., Nelson, R. D., Berg, E. L., Erlandsen, S. L. and Butcher, E. C. (1995). $\alpha 4$ integrins mediate lymphocyte attachment and rolling under physiologic flow. *Cell* **80**, 413-422.
- Chishima, T., Miyagi, Y., Wang, X., Yamaoka, H., Shimada, H., Moossa, A. R. and Hoffman R. M. (1997). Cancer invasion and micrometastasis visualized in live tissue by green fluorescent protein expression. *Cancer Res.* **57**, 2042-2047.
- Clark, R. A., Alon, R. and Springer, T. A. (1996). CD44 and hyaluronan-dependent rolling interactions of lymphocytes on tonsillar stroma. *J. Cell Biol.* **134**, 1075-1087.
- Davignon, D., Martz, E., Reynolds, T., Kürzinger, K. and Springer, T. A. (1981). Lymphocyte function-associated antigen 1 (LFA-1): a surface antigen distinct from Lyt-2,3 that participates in T lymphocyte-mediated killing. *Proc. Natl. Acad. Sci. USA* **78**, 4535-4539.
- de Alava, E., Panizo, A., Sola, I., Rodríguez-Rubio, F. I. and Pardo-Mindán, F. J. (1998). CD44v6 expression is related to progression in renal epithelial tumours. *Histopathology* **33**, 39-45.
- de Belder, A. N. and Wik, K. O. (1975). Preparation and properties of fluorescein-labelled hyaluronate. *Carbohydr. Res.* **44**, 251-257.
- DeGrendele, H. C., Estess, P., Picker, L. J. and Siegelman, M. H. (1996). CD44 and its ligand hyaluronate mediate rolling under physiologic flow: a novel lymphocyte-endothelial cell primary adhesion pathway. *J. Exp. Med.* **183**, 1119-1130.
- DeGrendele, H. C., Estess, P. and Siegelman M. H. (1997a). Requirement for CD44 in activated T cell extravasation into an inflammatory site. *Science* **278**, 672-675.
- DeGrendele, H. C., Kosfisz, M., Estess, P. and Siegelman M. H. (1997b). CD44 activation and associated primary adhesion is inducible via T cell receptor stimulation. *J. Immunol.* **159**, 2549-2553.
- DiMilla, P. A., Stone, J. A., Quinn, J. A., Albelda, S. M. and Lauffenburger, D. A. (1993). Maximal migration of human smooth muscle cells on fibronectin and type IV collagen occurs at an intermediate attachment strength. *J. Cell Biol.* **122**, 729-737.
- Duband, J. L., Nuckolls, G. H., Ishihara, A. and Hasegawa T. (1988). Fibronectin receptor exhibits high lateral mobility in embryonic locomoting cells but is immobile in focal contacts and fibrillar streaks in stationary cells. *J. Cell Biol.* **107**, 1385-1396.
- English, N., Lesley, J. and Hyman, R. (1998). Site-specific de-N-glycosylation of CD44 can activate hyaluronan binding and CD44 activation states show distinct threshold densities for hyaluronan binding. *Cancer Res.* **58**, 3736-3742.
- Estess, P., DeGrendele, H. C., Pascual, V. and Siegelman, M. H. (1998). Functional activation of lymphocyte CD44 in peripheral blood is a marker of autoimmune disease activity. *J. Clin. Invest.* **102**, 1173-1182.
- Fraser, J. R. E. and Laurent, T. C. (1989). Turnover and metabolism of hyaluronan. *Ciba Found. Symp.* **143**, 41-59.

- Gallatin, W. M., Weissman, I. L. and Butcher, E. C. (1983). A cell-surface molecule involved in organ-specific homing of lymphocytes. *Nature* **304**, 30-34.
- Günthert, U., Hoffmann, M., Rudy, W., Reber, S., Zöller, M., Haufmann, I., Matzku, S., Wenzel, A., Ponta, H. and Herrlich, P. (1991). A new variant of glycoprotein CD44 confers metastatic potential to rat carcinoma cells. *Cell* **65**, 13-24.
- Guo, Y.-J., Wong, J.-H., Lin, S.-C., Aruffo, A., Stamenkovic, I. and Sy, M.-S. (1994). Disruption of T lymphocyte reappearance in anti-Thy-1-treated animals in vivo with soluble CD44 and L-selectin molecules. *Cell Immunol.* **154**, 202-218.
- Herrlich, P., Rudy, W., Hofmann, M., Arch, R., Zöller, M., Zawadzki, V., Tölg, C., Hekele, A., Koopman, G., Pals, S. et al. (1993). CD44 and splice variants of CD44 in normal differentiation and tumor progression. In *Cell Adhesion Molecules* (ed. M. E. Hemler and E. Mihich), pp. 265-288. New York: Plenum Press.
- Ho, S. N., Hunt, H. D., Horton, R. M., Pullen, J. K. and Pease, L. R. (1989). Site-directed mutagenesis by overlap extension using the polymerase chain reaction. *Gene* **77**, 51-59.
- Ilangumaran, S., Borisch, B. and Hoessli, D. C. (1999). Signal transduction via CD44: role of plasma membrane microdomains. *Leuk. Lymphoma*. **35**, 455-469.
- Jones, M., Tussey, L., Athanasou, N. and Jackson, D. (2000). Heparan sulfate proteoglycan isoforms of the CD44 hyaluronan receptor induced in human inflammatory macrophages can function as paracrine regulators of fibroblast growth action. *J. Biol. Chem.* **275**, 7964-7974.
- Kastan, M. B., Onyekwere, O., Sidransky, D., Vogelstein, B. and Craig, R. W. (1991). Participation of p53 protein in the cellular response to DNA damage. *Cancer Res.* **51**, 6304-6311.
- Kurozumi, K., Nakao, K., Nishida, T., Nakahara, M., Ogino, N. and Tsujimoto, M. (1998). Significance of biologic aggressiveness and proliferating activity in papillary thyroid carcinoma. *World J. Surg.* **22**, 1237-1242.
- Lauffenburger, D. A. (1991). Models for receptor-mediated cell phenomena: adhesion and migration. *Annu. Rev. Biophys. Chem.* **20**, 387-414.
- Lawrence, M. B., Bainton, D. F. and Springer, T. A. (1994). Neutrophil tethering to and rolling on E-selectin are separable by requirement for L-selectin. *Immunity* **1**, 137-145.
- Lee, T. H., Wisniewski, H.-G. and Vilček, J. (1992). A novel secretory tumor necrosis factor-inducible protein (TSG-6) is a member of the family of hyaluronate binding proteins, closely related to the adhesion receptor CD44. *J. Cell Biol.* **116**, 545-557.
- Lesley, J., He, Q., Miyake, K., Hamann, A., Hyman, R. and Kincade, P. W. (1992). Requirements for hyaluronic acid binding by CD44: a role for the cytoplasmic domain and activation by antibody. *J. Exp. Med.* **175**, 257-266.
- Lesley, J., Hyman, R. and Kincade, P. W. (1993). CD44 and its interaction with extracellular matrix. *Adv. Immunol.* **54**, 271-335.
- Lesley, J., English, N., Perschl, A., Gregoroff, J. and Hyman, R. (1995). Variant cell lines selected for alterations in the function of the hyaluronan receptor CD44 show differences in glycosylation. *J. Exp. Med.* **182**, 431-437.
- Maloney, D. G., Kaminski, M. S., Burowski, D., Haimovich, J. and Levy, R. (1985). Monoclonal anti-idiotypic antibodies against the murine B cell lymphoma 38C13: characterization and use as probes for the biology of the tumor in vivo and in vitro. *Hybridoma* **4**, 191-209.
- Meredith, J. E., Jr and Schwartz, M. A. (1997). Integrins, adhesion and apoptosis. *Trends Cell Biol.* **7**, 146-150.
- Miyake, K., Medina, K. L., Hayashi, S.-I., Ono, S., Hamaoka, T. and Kincade, P. W. (1990). Monoclonal antibodies to Pgp-1/CD44 block lympho-hemopoiesis in long-term bone marrow cultures. *J. Exp. Med.* **171**, 477-488.
- Mohamadzadeh, M., DeGrendele, H., Arizpe, H., Estess, P. and Siegelman M. (1998). Proinflammatory stimuli regulate endothelial hyaluronan expression and CD44/HA-dependent primary adhesion. *J. Clin. Invest.* **101**, 97-108.
- Moll, J., Schmidt, A., van der Putten, H., Plug, R., Ponta, H., Herrlich, P. and Zöller, M. (1996). Accelerated immune response in transgenic mice expressing rat CD44v4-v7 on T cells. *J. Immunol.* **156**, 2085-2094.
- Naor, D., Vogt Sionov, R. and Ish-Shalom, D. (1997). CD44: structure, function, and association with the malignant process. *Adv. Cancer Res.* **71**, 241-319.
- Olifernko, S., Paiha, K., Harder, T., Gerke, V., Schwärzler, C., Schwarz, H., Beug, H., Günthert, U. and Huber, L. A. (1999). Analysis of CD44-containing lipid rafts: recruitment of Annexin II and stabilization by the actin cytoskeleton. *J. Cell Biol.* **146**, 843-854.
- Peach, R. J., Hollenbaugh, D., Stamenkovic, I. and Aruffo, A. (1993). Identification of hyaluronic acid binding sites in the extracellular domain of CD44. *J. Cell Biol.* **122**, 257-264.
- Rall, C. J. N. and Rustgi, A. K. (1995). CD44 isoform expression in primary and metastatic pancreatic adenocarcinoma. *Cancer Res.* **55**, 1831-1835.
- Rochman, M., Moll, J., Herrlich, P., Wallach, S. B., Nedvetzki, S., Vogt Sionov, R., Golan, I., Ish-Shalom, D. and Naor, D. (2000). The CD44 receptor of lymphoma cells: structure-function relationships and mechanism of activation. *Cell Adhes. Commun.* **7**, 331-347.
- Ruggiero, R. A., Bustuobad, O. D., Bonfil, R. D., Meiss, R. P. and Pasqualini, C. D. (1985). 'Concomitant immunity' in murine tumours of non-detectable immunogenicity. *Br. J. Cancer* **51**, 37-48.
- Salles, G., Zain, M., Jiang, W., Boussiotis, V. A. and Shipp, M. A. (1993). Alternatively spliced CD44 transcripts in diffuse large-cell lymphomas: characterization and comparison with normal activated B cells and epithelial malignancies. *Blood* **82**, 3539-3547.
- Sanchez-Madrid, F., Simon, P., Thompson, S. and Springer, T. A. (1983). Mapping of antigenic and functional epitopes on the α - and β -subunits of two related mouse glycoproteins involved in cell interactions, LFA-1 and MAC-1. *J. Exp. Med.* **158**, 586-602.
- Scott, J. E. (1961). The precipitation of polyanions by long-chain aliphatic ammonium salts. *Biochem. J.* **81**, 418-424.
- Screaton, G. R., Bell, M. V., Bell, J. I. and Jackson, D. G. (1993). The identification of a new alternative exon with highly restricted tissue expression in transcripts encoding the mouse Pgp-1 (CD44) homing receptor. Comparison of all 10 variable exons between mouse, human, and rat. *J. Biol. Chem.* **268**, 12235-12238.
- Sherman, L., Wainwright, D., Ponta, H. and Herrlich, P. (1998). A splice variant of CD44 expressed in the apical ectodermal ridge presents fibroblast growth factors to limb mesenchyme and is required for limb outgrowth. *Genes Dev.* **12**, 1058-1071.
- Skelton, T. P., Zeng, C., Nocks, A. and Stamenkovic, I. (1998). Glycosylation provides both stimulatory and inhibitory effects on cell surface and soluble CD44 binding to hyaluronan. *J. Cell Biol.* **140**, 431-446.
- Sleeman, J., Rudy, W., Hoffmann, M., Moll, J., Herrlich, P. and Ponta, H. (1996a). Regulated clustering of variant CD44 proteins increases their hyaluronate binding capacity. *J. Cell Biol.* **135**, 1139-1150.
- Sleeman, J. P., Arming, S., Moll, J. F., Hekele, A., Rudy, W., Sherman, L. S., Kreil, G., Ponta, H. and Herrlich, P. (1996b). Hyaluronate-independent metastatic behavior of CD44 variant-expressing pancreatic carcinoma cells. *Cancer Res.* **56**, 3134-3141.
- Sleeman, J. P., Kondo, K., Moll, J., Ponta, H. and Herrlich, P. (1997). Variant exons v6 and v7 together expand the repertoire of glycosaminoglycans bound by CD44. *J. Biol. Chem.* **272**, 31837-31844.
- Springer, T., Galfré, G., Secher, D. S. and Milstein, C. (1979). Mac-1: a macrophage differentiation antigen identified by monoclonal antibody. *Eur. J. Immunol.* **9**, 301-306.
- Springer, T. A. (1994). Traffic signals for lymphocyte recirculation and leukocyte emigration: the multistep paradigm. *Cell* **76**, 301-314.
- Stauder, R., Eisterer, W., Thaler, J. and Günthert, U. (1995). CD44 variant isoforms in non-Hodkin's lymphoma: a new independent prognostic factor. *Blood* **85**, 2885-2899.
- Sy, M.-S., Guo, Y.-J. and Stamenkovic, I. (1991). Distinct effects of two CD44 isoforms on tumor growth in vitro. *J. Exp. Med.* **174**, 859-866.
- Taher, E. I. T., Smit, L., Griffioen, A. W., Schilder-Tol, E. J. M., Borst, J. and Pals, S. T. (1996). Signaling through CD44 is mediated by tyrosine kinases. Association with p56^{lck} in T lymphocytes. *J. Biol. Chem.* **271**, 2863-2867.
- Takei, F. (1985). Inhibition of mixed lymphocyte response by a rat monoclonal antibody to a novel murine lymphocyte activation antigen (MALA-2). *J. Immunol.* **134**, 1403-1407.
- Tanaka, Y., Adams, D. H., Hubscher, S., Hirano, H., Siebenlist, U. and Shaw, S. (1993). T-cell adhesion induced by proteoglycan-immobilized cytokine MIP-1 β . *Nature* **361**, 79-82.
- Tempfer, C., Sliutz, G., Haeusler, G., Speiser, P., Reinthaller, A., Breitenecker, G., Vavra, N. and Kainz, Ch. (1998). CD44v3 and v6 variant isoform expression correlates with poor prognosis in early-stage vulvar cancer. *Br. J. Cancer* **78**, 1091-1094.
- Tian, B., Takasu, T. and Henke, C. (2000). Functional role of Cyclin A on induction of fibroblast apoptosis due to ligation of CD44 matrix receptor by anti-CD44 antibody. *Exp. Cell Res.* **257**, 135-144.

- Tölg, C., Hoffmann, M., Herrlich, P. and Ponta, H.** (1993). Splicing choice from ten variant exons establishes CD44 variability. *Nucleic Acids Res.* **21**, 1225-1229.
- Trowbridge, I. S., Lesley, J., Schulte, R., Hyman, R. and Trotter, J.** (1982). Biochemical characterization and cellular distribution of a polymorphic, murine cell-surface glycoprotein expressed on lymphoid tissues. *Immunogenetics* **15**, 299-312.
- van der Voort, R., Taher, T. E. I., Wielenga, V. J. M., Spaargaren, M., Prevo, R., Smit, L., David, G., Hartmann, G., Gherardi, E. and Pals, S. T.** (1999). Heparan sulfate-modified CD44 promotes hepatocyte growth factor/scatter factor-induced signal transduction through the receptor tyrosine kinase c-Met. *J. Biol. Chem.* **274**, 6499-6506.
- Vogt Sionov, R. and Naor, D.** (1997). Hyaluronan-independent lodgment of CD44⁺ lymphoma cells in lymphoid organs. *Int. J. Cancer* **71**, 462-469.
- Wallach, S. B., Friedmann, A. and Naor, D.** (2000). The CD44 receptor of the mouse LB T-cell lymphoma: Analysis of the isoform repertoire and ligand binding properties by reverse-transcriptase polymerase chain reaction and anti-sense oligonucleotides. *Cancer Detect. Prev.* **24**, 33-45.
- Weiss, J. M., Sleeman, J., Renkl, A. C., Dittmar, H., Termeer, C. C., Taxis, S., Howells, N., Hofmann, M., Köhler, G., Schöpf, E., Ponta, H., Herrlich, P. and Simon, J. C.** (1997). An essential role for CD44 variant isoforms in epidermal Langerhans cell and blood dendritic cell function. *J. Cell Biol.* **137**, 1137-1147.
- Weiss, L., Slavin, S., Reich, S., Cohen, P., Shuster, S., Stern, R., Kaganovsky, E., Okon, E., Rubinstein, A. M. and Naor, D.** (2000). Induction of resistance to diabetes in non-obese diabetic mice by targeting CD44 with a specific monoclonal antibody. *Proc. Natl. Acad. Sci. USA* **97**, 285-290.
- Yang, B., Yang, B. L. and Goetinck, P. F.** (1995). Biotinylated hyaluronic acid as a probe for identifying hyaluronic acid-binding proteins. *Anal. Biochem.* **228**, 299-306.
- Zahalka, M. A., Okon, E. and Naor, D.** (1993). Blocking lymphoma invasiveness with a monoclonal antibody directed against the β -chain of the leukocyte adhesion molecule (CD18). *J. Immunol.* **150**, 4466-4477.
- Zahalka, M. A., Okon, E., Gossler, U., Holzmann, B. and Naor, D.** (1995). Lymph node (but not spleen) invasion by murine lymphoma is both CD44- and hyaluronate-dependent. *J. Immunol.* **154**, 5345-5355.
- Zhou, D. F. H., Ding, J. F., Picker, L. J., Bargatze, R. F., Butcher, E. C. and Goeddel, D. V.** (1989). Molecular cloning and expression of Pgp-1. The mouse homolog of the human H-CAM (Hermes) lymphocyte homing receptor. *J. Immunol.* **143**, 3390-3395.